

# Combating Confirmation Bias: A Unified Pseudo-Labeling Framework for Entity Alignment

Qijie Ding<sup>1</sup>, Jie Yin<sup>1\*</sup>, Daokun Zhang<sup>2</sup>, Junbin Gao<sup>1</sup>

<sup>1</sup>Discipline of Business Analytics, The University of Sydney, Sydney, NSW, Australia.

<sup>2</sup>Department of Data Science & AI, Monash University, Melbourne, VIC, Australia.

\*Corresponding author(s). E-mail(s): [jie.yin@sydney.edu.au](mailto:jie.yin@sydney.edu.au);

Contributing authors: [qijie.ding@sydney.edu.au](mailto:qijie.ding@sydney.edu.au);

[daokun.zhang@monash.edu](mailto:daokun.zhang@monash.edu); [junbin.gao@sydney.edu.au](mailto:junbin.gao@sydney.edu.au);

## Abstract

Entity alignment (EA) aims at identifying equivalent entity pairs across different knowledge graphs (KGs) that refer to the same real-world identity. It has been a compelling but challenging task that requires the integration of heterogeneous information from different KGs to expand the knowledge coverage and enhance inference abilities. To circumvent the shortage of prior alignment seeds provided for training, recent EA models utilize pseudo-labeling strategies to iteratively add unaligned entity pairs predicted with high confidence to the training data for model retraining. However, the adverse impact of confirmation bias has been largely overlooked during pseudo-labeling, thus hindering entity alignment performance. To systematically combat confirmation bias, we propose a Unified Pseudo-Labeling framework for Entity Alignment (UPL-EA) that explicitly eliminates pseudo-labeling errors to boost the accuracy of entity alignment. UPL-EA consists of two complementary components: (1) The Optimal Transport (OT)-based pseudo-labeling uses discrete OT modeling as an effective means to enable more accurate determination of entity correspondences across two KGs and to mitigate the adverse impact of erroneous matches. A simple but highly effective criterion is further devised to derive pseudo-labeled entity pairs that satisfy one-to-one correspondences at each iteration. (2) The cross-iteration pseudo-label calibration operates across multiple consecutive iterations to further improve the pseudo-labeling precision rate by reducing the local pseudo-label selection variability with a theoretical guarantee. The two components are respectively designed to eliminate Type I and Type II pseudo-labeling errors identified through our analyse. The calibrated pseudo-labels are thereafter used to augment

prior alignment seeds to reinforce subsequent model training for alignment inference. The effectiveness of UPL-EA in eliminating pseudo-labeling errors is both theoretically supported and experimentally validated. The experimental results show that our approach achieves competitive performance with limited prior alignment seeds.

**Keywords:** Entity Alignment, Pseudo-labeling, Optimal Transport, Knowledge Graphs

## 1 Introduction

Knowledge Graphs (KGs) are large-scale structured knowledge bases that represent real-world entities (or concepts) and their relationships as a collection of factual triplets. Recent years have witnessed the release of various open-source KGs (e.g., Freebase (Bollacker et al, 2008), YAGO (Suchanek et al, 2007) and Wikidata (Vrandečić and Krötzsch, 2014)) from general to specific domains and their proliferation to empower many artificial intelligence (AI) applications, such as recommender systems (Guo et al, 2022), question answering (Yang et al, 2018) and information retrieval (Paulheim, 2017). Nevertheless, it has become a well-known fact that real-world KGs suffer from incompleteness arising from their complex, semi-automatic construction process. This has led to an increasing number of research efforts on knowledge graph completion, such as TransE (Bordes et al, 2013) and TransH (Wang et al, 2014), which aim to add missing facts to individual KGs. Unfortunately, due to its limited coverage and incompleteness, a single KG cannot fulfill the requirements for complex AI applications that build upon heterogeneous knowledge sources. This necessitates the integration of heterogeneous information from multiple individual KGs to enrich knowledge representation. Entity alignment (EA) is a crucial task towards this objective, which aims to establish the correspondence between equivalent entity pairs across different KGs that refer to the same real-world identity.

Over the last decade, there has been a surge of research efforts dedicated to entity alignment across KGs. Most mainstream entity alignment models are based on knowledge graph embedding, which embeds different KGs into a common latent space so that similarities between entities can be directly measured via their embeddings for alignment purposes. To learn better KG embeddings, methods like GCN-Align (Wang et al, 2018) leverage graph convolutional networks (GCNs) (Kipf and Welling, 2017) to capture structural and neighboring entity information for alignment inference. Along this line of research, recent studies (Wu et al, 2019b,a; Zhu et al, 2021) utilize a highway strategy (Srivastava et al, 2015) to alleviate over-smoothing during GCN propagation, or jointly learn entity and relation embeddings for improving the accuracy of entity alignment. These models, however, require an abundant amount of pre-aligned entity pairs (known as *prior alignment seeds*) during training, which are labor-intensive and costly to acquire in real-world KGs. To tackle the shortage of prior alignment seeds provided for training, recently proposed models, such as BootEA (Sun et al, 2018), IPTransE (Zhu et al, 2017), MRAEA (Mao et al, 2020), and RNM (Zhu et al, 2021), adopt a bootstrapping strategy that iteratively selects unaligned entity pairs predicted

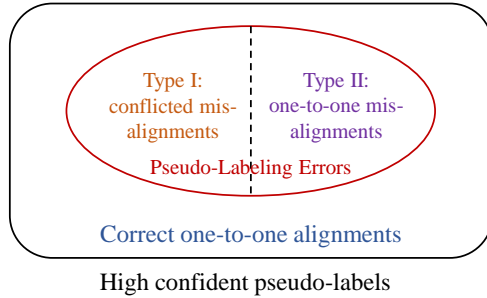


**Fig. 1:** The composition of pseudo-labels generated based on the model’s high confidence predictions. The resultant pseudo-labeling errors comprise Type I errors (conflicted misalignments) and Type II errors (one-to-one misalignments).

with high confidence as pseudo-labels and adds them to prior alignment seeds for either model re-training or posterior embedding distance rectification. The bootstrapping strategy originates from the field of statistics and is also referred to as pseudo-labeling – a predominant learning paradigm proposed to tackle the label scarcity problem in semi-supervised learning.

In general semi-supervised learning, pseudo-labeling approaches inherently suffer from confirmation bias (Arazo et al, 2020; Tarvainen and Valpola, 2017). The bias stems from using incorrectly predicted labels generated on unlabeled data for subsequent training, thereby misleadingly increasing confidence in incorrect predictions and generating a biased model with degraded performance. Unfortunately, there is a lack of understanding of the fundamental factors that give rise to confirmation bias for pseudo-labeling-based entity alignment. Our analysis (see Section 2.2) advocates that the confirmation bias is exacerbated during pseudo-labeling for entity alignment. Due to the lack of sufficient prior alignment seeds at the early stages of training, the existing models are inclined to learn uninformative entity embeddings and make incorrect predictions on unaligned entity pairs. As a consequence, the pseudo-labels generated based on the model’s unreliable high-confidence predictions are error-prone. The resultant errors can be characterized into two types, as depicted in Fig. 1. **Type I pseudo-labeling errors** refer to *conflicted misalignments*, where a single entity in one KG is simultaneously aligned with multiple entities in another KG with erroneous matches. **Type II pseudo-labeling errors** refer to *one-to-one misalignments*, where an entity in one KG is incorrectly matched with an entity in another KG. These pseudo-labeling errors, if not properly mitigated, would propagate into subsequent model training, thereby jeopardizing the efficacy of pseudo-labeling-based entity alignment. However, current pseudo-labeling-based EA models have made only limited attempts to alleviate alignment conflicts using simple heuristics (Zhu et al, 2021; Mao et al, 2020) or imposing constraints to enforce hard alignments (Sun et al, 2018; Ding et al, 2022), while the confirmation bias has been left under-explored.

To fill in the research gap, in this work, we propose a Unified Pseudo-Labeling framework for Entity Alignment (UPL-EA) to systematically combat confirmation bias. The scope of our work focuses primarily on a semi-supervised learning paradigm,

where we aim to eliminate Type I and Type II pseudo-labeling errors to boost the precision of entity alignment. Towards this goal, UPL-EA comprises two complementary components – within-iteration Optimal Transport (OT)-based pseudo-labeling and cross-iteration pseudo-label calibration. Specifically, OT-based pseudo-labeling uses discrete OT modeling as an effective means to enable more accurate determination of entity correspondences across KGs and to mitigate the adverse impact of erroneous matches. The discrete OT models the alignment as a probabilistic matching process between the entity sets in two KGs with the minimal overall transport cost. The transport cost is calculated according to the rectified distance between entity embeddings obtained through graph convolution augmented with global-level semantics. Based on the estimated OT solution, a simple but highly effective selection criterion is further devised to infer pseudo-labeled entity pairs that satisfy one-to-one correspondence, thus eliminating conflicted misalignments (Type I pseudo-labeling errors) at each iteration. The pseudo-label calibration operates across multiple consecutive iterations to reduce the local pseudo-label selection variability with theoretical guarantee, thereby eliminating one-to-one misalignments (Type II pseudo-labeling errors). The calibrated pseudo-labels are then used to augment prior alignment seeds to reinforce subsequent model training for alignment inference.

The contribution of this paper can be summarized as follows:

- To our best knowledge, we are the first to investigate the confirmation bias problem for pseudo-labeling-based entity alignment. We conceptually and empirically identify two types of pseudo-labeling errors that give rise to confirmation bias.
- Motivated by our analysis, we propose a unified pseudo-labeling framework (UPL-EA) that systematically alleviates the problem of confirmation bias for pseudo-labeling-based entity alignment. UPL-EA is carefully designed to explicitly eliminate Type I and Type II pseudo-labeling errors, leading to significant performance gains.
- Extensive experiments on benchmark KG datasets demonstrate that UPL-EA is able to significantly eliminate pseudo-labeling errors and yield competitive performance with respect to limited amounts of prior alignment seeds, outperforming state-of-the-art supervised and semi-supervised baselines.

The remainder of this paper is organized as follows. Section 2 provides a problem formulation of pseudo-labeling-based entity alignment and presents an empirical analysis of confirmation bias that motivates this work. Section 3 presents the proposed framework, followed by extensive experimental evaluation reported in Section 4. Related works are discussed in Section 5, and we conclude the paper in Section 6.

## 2 Preliminaries

In this section, we first provide a problem formulation of pseudo-labeling-based entity alignment. Then, we perform a thorough analysis of confirmation bias during pseudo-labeling, which motivates the design of our proposed framework.

## 2.1 Problem Formulation

A knowledge graph (KG) can be defined as  $\mathcal{G} = \{\mathcal{E}, \mathcal{R}, \mathcal{T}\}$  with the entity set  $\mathcal{E}$ , relation set  $\mathcal{R}$ , and triplet set  $\mathcal{T}$ . We use  $e \in \mathcal{E}$ ,  $r \in \mathcal{R}$ ,  $(e_i, r, e_j) \in \mathcal{T}$  to represent an entity, a relation, and a triplet, respectively. Each entity  $e$  is characterized by an attribute vector  $\mathbf{x}_e$ , which can be obtained from entity names with semantic meanings or entity textual descriptions. Formally, two heterogeneous KGs are given for the task of entity alignment, i.e.,  $\mathcal{G}_1 = \{\mathcal{E}_1, \mathcal{R}_1, \mathcal{T}_1\}$  and  $\mathcal{G}_2 = \{\mathcal{E}_2, \mathcal{R}_2, \mathcal{T}_2\}$ . An entity  $e_i \in \mathcal{E}_1$  in  $\mathcal{G}_1$  is likely to correspond to the same concept with another entity  $e_j \in \mathcal{E}_2$  in  $\mathcal{G}_2$ , denoted as  $e_i \Leftrightarrow e_j$ , and vice versa.

To provide supervision for entity alignment, a small number of pre-aligned entity pairs between  $\mathcal{G}_1$  and  $\mathcal{G}_2$  are sometimes provided as prior alignment seeds in the form of  $\mathcal{L}_e^0 = \{(e_i, e_j) \mid e_i \in \mathcal{E}_1, e_j \in \mathcal{E}_2, e_i \Leftrightarrow e_j\}$ . Apart from prior alignment seeds, there are two sets of unaligned entities  $\mathcal{E}'_1 \subseteq \mathcal{E}_1$  and  $\mathcal{E}'_2 \subseteq \mathcal{E}_2$  respectively from two KGs.

Given two KGs,  $\mathcal{G}_1$  and  $\mathcal{G}_2$ , the task of *pseudo-labeling-based entity alignment* iterates over the following two components: (1) Training an entity alignment (EA) model that learns entity embeddings  $f_\theta(\mathcal{L}_e) : \mathbf{h}_e \rightarrow \mathbb{R}^d$  using the available alignment seeds  $\mathcal{L}_e$ , where  $\mathcal{L}_e$  is set to the prior alignment seeds  $\mathcal{L}_e^0$  at the first iteration,  $e \in \mathcal{E}_1 \cup \mathcal{E}_2$ , and  $d$  is the embedding dimension; (2) Designing a pseudo-label selection component that selects unaligned entity pairs  $g(\mathbf{h}_{e_i}, \mathbf{h}_{e_j}) : \mathcal{E}'_1 \times \mathcal{E}'_2 \rightarrow \{0, 1\}$  using learned entity embeddings  $\mathbf{h}_e$ , then augments alignment seeds with pseudo-labels, i.e.,  $\mathcal{L}_e \leftarrow \mathcal{L}_e \cup \{(e_i, e_j) \mid e_i \in \mathcal{E}'_1, e_j \in \mathcal{E}'_2, g(\mathbf{h}_{e_i}, \mathbf{h}_{e_j}) = 1\}$ .

To achieve accurate entity alignment, we need to ensure that: (1) the EA model  $f_\theta$  has the capacity to learn informative, high-quality entity embeddings; (2) the pseudo-label selection component  $g$  can select precise pseudo-labeled entity pairs for augmenting alignment seeds, providing high-quality supervision for boosting the EA model. The two components reinforce each other alternately to make accurate inferences for entity alignment.

## 2.2 Analysis of Confirmation Bias

To investigate the impact of confirmation bias on pseudo-labeling-based entity alignment, we perform an error analysis of a naive pseudo-labeling strategy, where unaligned entity pairs with an embedding distance smaller than a pre-specified threshold are selected as pseudo-labels. To gain insights into the underlying causes of confirmation bias, we explicitly analyze the variations in Type I and Type II pseudo-labeling errors throughout the training process, when the naive pseudo-labeling strategy is used. This analysis is conducted on a widely used cross-lingual benchmark dataset DBP15K<sub>ZH\_EN</sub> (Sun et al, 2017) (Details of the dataset are presented in Section 4.1). We follow the conventional 30%-70% ratio to randomly split the training and test data on the 15,000 ground truth entity alignment pairs provided. The proportions of two types of errors and entity alignment accuracy are calculated at different iterations on the test data. As shown in Fig. 2a, Type I and Type II pseudo-labeling errors could propagate and increase proportionally via the naive pseudo-labeling strategy as training proceeds. The accumulated errors give rise to confirmation bias, thereby severely hindering the capability of pseudo-labeling for performance improvements.

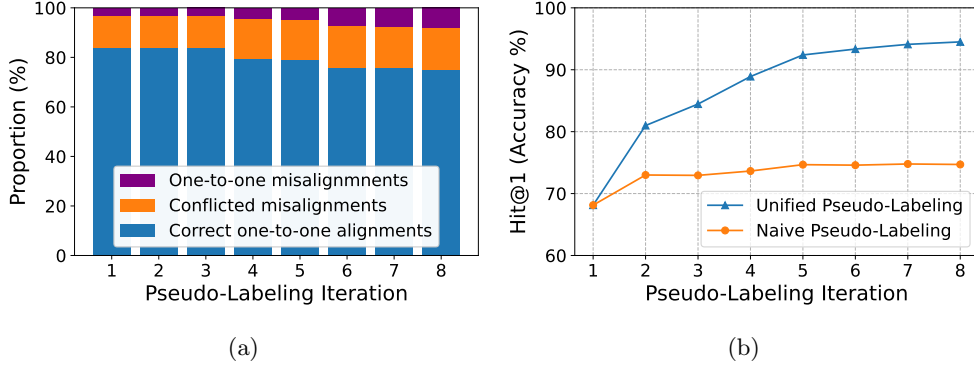


**Fig. 2:** Error analysis of confirmation bias. (a) Proportion of pseudo-labels selected by a naive pseudo-labeling strategy over training iterations. (b) Entity alignment accuracy of the naive pseudo-labeling strategy and the proposed unified pseudo-labeling strategy over training iterations.

Our analysis affirms that the confirmation bias essentially stems from Type I and Type II pseudo-labeling errors. These errors, if not adequately addressed, would propagate into subsequent model training, thus diminishing the effectiveness of pseudo-labeling for entity alignment. Our work is thus motivated to explicitly eliminate Type I and Type II pseudo-labeling errors, leading to significant performance improvements for entity alignment inference. As shown in Fig. 2b, our proposed method outperforms the naive pseudo-labeling strategy, yielding substantial performance gains.

### 3 The Proposed UPL-EA Framework

With the insights derived from our analysis in Section 2.2, the proposed UPL-EA framework is designed to systematically address the confirmation bias issue for pseudo-labeling based entity alignment. At the core of UPL-EA are two key complementary modules that greatly enhance the entity alignment (EA) model:

- Module 1 (Within-Iteration OT-Based Pseudo-Labeling) utilizes Optimal Transport (OT) modeling to more precisely determine the correspondences between entities across KGs so as to eliminate conflicted misalignments at each iteration. (**Addressing Type I pseudo-labeling errors**)
- Module 2 (Cross-Iteration Pseudo-Label Calibration) further calibrates pseudo-labels generated from Module 1 across iterations to reduce local variability of pseudo-label selection so as to minimize one-to-one misalignments across iterations. (**Addressing Type II pseudo-labeling errors**)

Fig. 3 illustrates an overview of the proposed UPL-EA framework. At each iteration, the EA model learns informative entity embeddings via a global-local aggregation scheme based on the available alignment seeds. Then, Module 1 takes entity embeddings as input to pseudo-label conflict-free entity alignment pairs (eliminating Type I

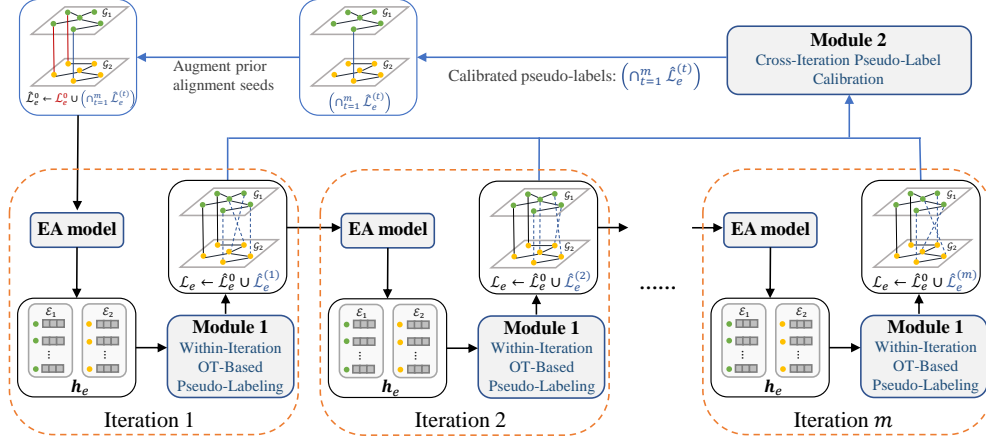


**Fig. 3:** The overall framework of the proposed UPL-EA model.

pseudo-labeling errors), which are further used by the EA model in the subsequent iteration. After every  $m$  iterations, pseudo-labels across iterations are passed on to Module 2 for further calibration, preventing one-to-one misalignments (Type II pseudo-labeling errors) from accumulating in subsequent model training. The calibrated pseudo-labels are then used to augment the prior alignment seeds. The augmented alignment seeds are used by the next  $m$  iterations to perform pseudo-labeling-based entity alignment. The EA model and the pseudo-label selection component empowered by Module 1 and Module 2 mutually reinforce each other to learn informative entity embeddings. Lastly, the learned entity embeddings are used for entity alignment inference.

### 3.1 Entity Alignment Model

The entity alignment (EA) model aims to learn informative entity embeddings and perform model training for entity alignment inference.

#### 3.1.1 Global-Local Aggregation for Entity Embedding Learning

To enable the EA model to learn informative entity embeddings, it is essential to capture the relational information conveyed in KGs. Towards this end, we employ a global-local aggregation scheme (Ding et al, 2022) to perform two levels of neighborhood aggregation for each entity in  $\mathcal{G}_1$  and  $\mathcal{G}_2$ .

**Global-Level Relation Aggregation.** To capture the global statistics of a given relation  $r_i$ , we construct its feature vector  $\mathbf{x}_{r_i}$  by taking into account all triplets associated with  $r_i$  in two KGs. To be specific, we compute the feature vector  $\mathbf{x}_{r_i}$  for each relation  $r_i \in \mathcal{R}_1 \cup \mathcal{R}_2$ , by taking an average of the concatenated feature vectors of its associated head and tail entities:

$$\mathbf{x}_{r_i} = \frac{1}{|\{(e_h, r_i, e_t) \in \mathcal{T}_1 \cup \mathcal{T}_2\}|} \sum_{(e_h, r_i, e_t) \in \mathcal{T}_1 \cup \mathcal{T}_2} [\mathbf{x}_{e_h} \parallel \mathbf{x}_{e_t}], \quad (1)$$

where  $[\cdot|\cdot]$  denotes the concatenation operation,  $\{(e_h, r_i, e_t) \in \mathcal{T}_1 \cup \mathcal{T}_2\}$  is the set of all triplets associated with relation  $r_i$ .  $\mathbf{x}_{e_h}$  and  $\mathbf{x}_{e_t} \in \mathbb{R}^d$  are the feature vectors of entity  $e_h$  and  $e_t$ , respectively. As such, the obtained relation feature vector  $\mathbf{x}_{r_i} \in \mathbb{R}^{2d}$  can capture the intrinsic relational semantics of relation  $r_i$ . Then, for each entity  $e_i \in \mathcal{E}_1 \cup \mathcal{E}_2$ , we construct its averaged neighboring relation feature as follows:

$$\mathbf{x}_{e_i-rels} = \frac{1}{|\mathcal{N}_r(e_i)|} \sum_{r_j \in \mathcal{N}_r(e_i)} \mathbb{I}_{e_i}(r_j) \cdot \mathbf{x}_{r_j}, \quad (2)$$

where  $\mathcal{N}_r(e_i)$  is the set of one-hop neighboring relations of entity  $e_i$ .  $\mathbb{I}_{e_i}(r_j)$  indicates the direction of relation  $r_j$  with respect to  $e_i$ , where  $-1$  indicates the successor of  $e_i$  and  $+1$  indicates the predecessor of  $e_i$ . The incorporation of directional information enables to capture richer relational information in the neighborhood, benefiting the learning of entity embeddings.

To perform global-level relation aggregation, we concatenate each entity’s averaged neighboring relation feature  $\mathbf{x}_{e_i-rels} \in \mathbb{R}^{2d}$  with its original feature  $\mathbf{x}_{e_i} \in \mathbb{R}^d$ , followed by a non-linear transformation to capture the interplay between different dimensions:

$$\tilde{\mathbf{h}}_{e_i}^{(1)} = \text{ReLU}(W_1[\mathbf{x}_{e_i} \parallel \mathbf{x}_{e_i-rels}] + b_1), \quad (3)$$

where  $\text{ReLU}(\cdot)$  is the ReLU activation function,  $W_1 \in \mathbb{R}^{d \times 3d}$  and  $b_1 \in \mathbb{R}^d$  are the weight matrix and the bias vector, respectively. To avoid over-smoothing and deliver a more effective representation scheme, we augment the embedding vector  $\tilde{\mathbf{h}}_{e_i}^{(1)}$  with the original entity feature vector  $\mathbf{x}_{e_i}$ :

$$\mathbf{h}_{e_i}^{(1)} = \tilde{\mathbf{h}}_{e_i}^{(1)} + \mathbf{x}_{e_i}. \quad (4)$$

**Local-Level Entity Aggregation.** After obtaining entity embeddings via relation aggregation at the global level, we further perform local-level entity aggregation to capture neighboring entity structures.

For this purpose, we take advantage of a two-layer GCN (Kipf and Welling, 2017) along with a highway gate strategy (Srivastava et al, 2015) to avoid over-smoothing. Formally, we first stack relation aggregated entity embeddings  $\mathbf{h}_{e_i}^{(1)}$  for each entity  $e_i \in \mathcal{E}_1 \cup \mathcal{E}_2$  into an embedding matrix  $H_e^{(1)} \in \mathbb{R}^{(|\mathcal{E}_1|+|\mathcal{E}_2|) \times d}$ , where each row indicates the embedding vector of the corresponding entity. Then, the entity embedding matrix  $H_e^{(1)}$  is updated as follows from  $l = 1$ :

$$\begin{cases} \tilde{H}_e^{(l+1)} = \text{ReLU}(\tilde{D}^{-\frac{1}{2}} \tilde{A} \tilde{D}^{-\frac{1}{2}} H_e^{(l)} W_{l+1}), \\ H_e^{(l+1)} = T(H_e^{(l)}) \odot \tilde{H}_e^{(l+1)} + (1 - T(H_e^{(l)})) \odot H_e^{(l)}. \end{cases} \quad (5)$$

Above,  $\tilde{A} = A + I_{|\mathcal{E}_1|+|\mathcal{E}_2|}$  denotes the undirected adjacency matrix of the combined graph  $\mathcal{G}_1 \cup \mathcal{G}_2$  with self-connections that are represented by the  $(|\mathcal{E}_1|+|\mathcal{E}_2|) \times (|\mathcal{E}_1|+|\mathcal{E}_2|)$  identity matrix  $I_{|\mathcal{E}_1|+|\mathcal{E}_2|}$ .  $\tilde{D}_{ii} = \sum_j \tilde{A}_{ij}$  is the degree matrix,  $W_{l+1} \in \mathbb{R}^{d \times d}$  is the



weight matrix at layer  $l$ , and  $\odot$  is the Hadamard product (or element-wise multiplication). In addition,  $T(H_e^{(l)}) = \sigma(H_e^{(l)} W_T^{(l)} + b_T^{(l)}) \in \mathbb{R}^{(|\mathcal{E}_1|+|\mathcal{E}_2|) \times d}$  is the transformation gate obtained from  $H_e^{(l)}$ , where  $\sigma(\cdot)$  is the Sigmoid activation function,  $W_T^{(l)} \in \mathbb{R}^{d \times d}$  and  $b_T^{(l)} \in \mathbb{R}^d$  are the gate-specific weight matrix and bias vector, respectively. The transformation gate helps filter out the over-smoothed feature dimensions.

Finally, the entity embedding matrix is obtained as  $H_e^{(3)}$ . Accordingly, the final embedding for entity  $e_i$  is  $\mathbf{h}_{e_i} = \mathbf{h}_{e_i}^{(3)} \in \mathbb{R}^d$ , where  $\mathbf{h}_{e_i}^{(3)} \in \mathbb{R}^d$  is the transpose of the row vector of  $H_e^{(3)}$  indexed by entity  $e_i$ .

### 3.1.2 Model Training for Entity Alignment

Given a set of alignment seeds  $\mathcal{L}_e$  together the constructed entity embeddings, the loss function for entity alignment can be defined as:

$$L = \sum_{(e_i, e_j) \in \mathcal{L}_e} \sum_{(e_{i'}, e_{j'}) \in \mathcal{L}'_e} \hat{R}(e_i, e_j) \cdot \max(0, d(e_i, e_j) - d(e_{i'}, e_{j'}) + \gamma), \quad (6)$$

where  $\mathcal{L}'_e$  is the set of sampled negative alignment pairs that are not included in  $\mathcal{L}_e$ .  $\gamma$  is a hyper-parameter that determines the margin to separate positive pairs from negative pairs.  $d(e_i, e_j)$  indicates the embedding distance between entity pair  $(e_i, e_j)$  across two KGs, defined as:

$$d(e_i, e_j) = \|\mathbf{h}_{e_i} - \mathbf{h}_{e_j}\|_1. \quad (7)$$

Above,  $\hat{R}(e_i, e_j)$  indicates a weighting factor that measures distinct contribution of each alignment pair  $(e_i, e_j)$  to the overall loss. For any pair from the prior alignment seeds,  $\hat{R}(e_i, e_j) = 1$ , otherwise  $\hat{R}(e_i, e_j) = 1/(1 + e^{\tilde{d}(e_i, e_j)}) \in (0, 1)$ , where  $\tilde{d}(e_i, e_j)$  denotes the rectified embedding distance defined later using Eq.(8) in Section 3.2.

For model training, we adopt an *adaptive negative sampling* strategy to obtain a negative alignment set  $\mathcal{L}'_e$ . Specifically, for each positive pair  $(e_i, e_j)$  in the alignment set  $\mathcal{L}_e$ , we select  $K$  nearest entities of  $e_i$  (or  $e_j$ ) measured by the embedding distance in Eq. (7) to replace  $e_j$  (or  $e_i$ ) and form  $K$  negative counterparts  $(e_i, e_{j'})$  (or  $(e_{i'}, e_j)$ ). This adaptive strategy helps produce ‘‘hard’’ negative alignment pairs and push their associated entities to be apart from each other in the embedding space.

After minimizing the loss on the set of alignment seeds, the learned entity embeddings  $\mathbf{h}_e$  can be used to infer unaligned entity pairs as pseudo-labels, which are used to augment alignment seeds for subsequent training. However, as we have discussed earlier in Section 2.2, using a naive pseudo-label selection strategy would inevitably result in a large portion of erroneous pseudo-labels in the form of Type I and Type II pseudo-labeling errors, leading to confirmation bias.

Below, we detail the two key modules that are explicitly proposed to mitigate Type I and Type II pseudo-labeling errors, respectively.

### 3.2 Within-Iteration OT-Based Pseudo-Labeling

To effectively mitigate Type I pseudo-labeling errors, we propose to use Optimal Transport (OT) as an effective means to more precisely determine one-to-one correspondence between entities across KGs. This ensures that correct entity alignment pairs can be sufficiently pseudo-labeled at each iteration to boost entity alignment performance significantly.

The within-iteration OT-based pseudo-labeling module uses the distances between the learned entity embeddings to define the transport cost for OT-based modeling. However, directly employing the original embedding distances would be error-prone, especially at early training stages where the learned entity embeddings are uninformative. Thus, we resort to rectifying the embedding distance defined in Eq. (7) using relational neighborhood matching (Zhu et al, 2021).

The principle of distance rectification is to leverage the relational context within local neighborhoods to aid in determining the extent to which two entities should be aligned. Intuitively, if two entities  $e_i \in \mathcal{E}_1$  and  $e_j \in \mathcal{E}_2$  share more aligned neighboring relations/entities, the distance between their embeddings should be smaller, and thus they are more likely to be aligned with each other. As such, the embedding distance used for pseudo-labeling is rectified as

$$\tilde{d}(e_i, e_j) = d(e_i, e_j) - \lambda s(e_i, e_j), \quad (8)$$

where  $\lambda$  is a trade-off parameter,  $s(e_i, e_j)$  is a score function indicating the degree to which relational contexts of two entities match. It is calculated by determining whether neighboring entities/relations between  $(e_i, e_j)$  are aligned or not:

$$s(e_i, e_j) = \left( \sum_{\mathcal{M}_{e_i, e_j}} \frac{1}{|\{e | (e, r, e_k) \in \mathcal{T}_1\}| \cdot |\{e | (e, r', e_l) \in \mathcal{T}_2\}|} \right) / (|\mathcal{N}_e(e_i)| + |\mathcal{N}_e(e_j)|), \quad (9)$$

where  $\mathcal{M}_{e_i, e_j}$  is the set of matched neighboring relation-entity tuples:

$$\mathcal{M}_{e_i, e_j} = \{(e_k, e_l, r, r') | e_k \in \mathcal{N}_e(e_i), e_l \in \mathcal{N}_e(e_j), (e_i, r, e_k) \in \mathcal{T}_1, (e_j, r', e_l) \in \mathcal{T}_2, (e_k, e_l) \in \mathcal{L}_e, (r, r') \in \mathcal{L}_r\}, \quad (10)$$

$\mathcal{N}_e(e)$  is the set of neighboring entities of entity  $e$ .  $\mathcal{L}_r$  is the set of aligned relations obtained via pseudo-labeling based on the embedding distance between relations.

Moreover, due to the smoothing effect of feature aggregation, entities in the neighborhood tend to have indistinguishable representations. As a result, simply using a pre-specified threshold to pseudo-label entity pairs would inevitably result in conflicted misalignments. To circumvent this issue, we propose an OT-based strategy to discover a globally optimal alignment configuration with minimal overall inconsistency.

To warrant one-to-one alignments, we model the alignment between two unaligned sets  $\mathcal{E}'_1$  and  $\mathcal{E}'_2$  as an OT process, i.e., transporting each entity  $e_i \in \mathcal{E}'_1$  to a unique entity  $e_j \in \mathcal{E}'_2$ , with minimal overall transport cost. Naturally, the rectified distance

can be used to define the transport cost across two KGs:

$$C_{e_i, e_j} = \tilde{d}(e_i, e_j), \quad e_i \in \mathcal{E}'_1, e_j \in \mathcal{E}'_2, \quad (11)$$

where  $C \in \mathbb{R}^{|\mathcal{E}'_1| \times |\mathcal{E}'_2|}$  is the transport cost matrix. Without loss of generality, we assume  $|\mathcal{E}'_1| < |\mathcal{E}'_2|$ . The transport plan is a mapping function  $T : e_i \rightarrow T(e_i)$ , where  $e_i \in \mathcal{E}'_1, T(e_i) \in \mathcal{E}'_2$ . The objective is thus to find the optimal transport plan  $T^*$  that minimizes the overall transport cost:

$$T^* = \arg \min_T \sum_{e_i \in \mathcal{E}'_1} C_{e_i, T(e_i)}. \quad (12)$$

Eq. (12) models a hard assignment optimization problem that is not scaled up. To enable more efficient optimization and to allow for a more flexible alignment configuration, we reformulate this objective as a discrete OT problem, where the optimal transport plan is considered as a coupling matrix  $P^* \in \mathbb{R}_+^{|\mathcal{E}'_1| \times |\mathcal{E}'_2|}$  between two discrete distributions. We denote  $\boldsymbol{\mu}$  and  $\boldsymbol{\nu}$  as two discrete probability distributions over all entities  $\{e_i | e_i \in \mathcal{E}'_1\}$  and  $\{e_j | e_j \in \mathcal{E}'_2\}$ , respectively. Without any entity alignment preference, the two discrete distributions  $\boldsymbol{\mu}$  and  $\boldsymbol{\nu}$  are assumed to follow a uniform distribution such that  $\boldsymbol{\mu} = \frac{1}{|\mathcal{E}'_1|} \sum_{e_i \in \mathcal{E}'_1} \delta_{e_i}$  and  $\boldsymbol{\nu} = \frac{1}{|\mathcal{E}'_2|} \sum_{e_j \in \mathcal{E}'_2} \delta_{e_j}$ , where  $\delta_{e_i}$  and  $\delta_{e_j}$  are the Dirac function centered on  $e_i$  and  $e_j$ , respectively. Both  $\boldsymbol{\mu}$  and  $\boldsymbol{\nu}$  are bounded to sum up to one:  $\sum_{e_i \in \mathcal{E}'_1} \boldsymbol{\mu}(e_i) = \sum_{e_i \in \mathcal{E}'_1} \frac{1}{|\mathcal{E}'_1|} = 1$  and  $\sum_{e_j \in \mathcal{E}'_2} \boldsymbol{\nu}(e_j) = \sum_{e_j \in \mathcal{E}'_2} \frac{1}{|\mathcal{E}'_2|} = 1$ . Accordingly, the OT objective is formulated as finding the optimal coupling matrix  $P^*$  between  $\boldsymbol{\mu}$  and  $\boldsymbol{\nu}$ :

$$\begin{aligned} P^* &= \arg \min_{P \in \Pi(\boldsymbol{\mu}, \boldsymbol{\nu})} \sum_{e_i \in \mathcal{E}'_1} \sum_{e_j \in \mathcal{E}'_2} P_{e_i, e_j} \cdot C_{e_i, e_j}, & (13) \\ \text{subject to: } & \sum_{e_j \in \mathcal{E}'_2} P_{e_i, e_j} = \boldsymbol{\mu}(e_i) = \frac{1}{|\mathcal{E}'_1|}, \\ & \sum_{e_i \in \mathcal{E}'_1} P_{e_i, e_j} = \boldsymbol{\nu}(e_j) = \frac{1}{|\mathcal{E}'_2|}, \\ & P_{e_i, e_j} \geq 0, \forall e_i \in \mathcal{E}'_1, \forall e_j \in \mathcal{E}'_2, \end{aligned}$$

where  $\Pi(\boldsymbol{\mu}, \boldsymbol{\nu}) = \{P \in \mathbb{R}_+^{|\mathcal{E}'_1| \times |\mathcal{E}'_2|} | P \mathbf{1}_{|\mathcal{E}'_2|} = \boldsymbol{\mu}, P^\top \mathbf{1}_{|\mathcal{E}'_1|} = \boldsymbol{\nu}\}$  is the set of all joint probability distributions with marginal probabilities  $\boldsymbol{\mu}$  and  $\boldsymbol{\nu}$ ,  $\mathbf{1}_n$  denotes an  $n$ -dimensional vector of ones.  $P$  is a coupling matrix signifying probabilistic alignments between two unaligned entity sets  $\mathcal{E}'_1$  and  $\mathcal{E}'_2$ . Therefore,  $P_{e_i, e_j}$  indicates the amount of probability mass transported from  $\boldsymbol{\mu}(e_i)$  to  $\boldsymbol{\nu}(e_j)$ . A larger value of  $P_{e_i, e_j}$  indicates a higher likelihood of  $e_i$  and  $e_j$  being aligned to each other.

To solve this discrete OT problem, some exact algorithms have been proposed, such as interior point methods (Wächter and Biegler, 2006) and network simplex (Orlin, 1997). The exact algorithms guarantee finding a closed-form optimal transport plan but with considerably high computational cost, making them intractable to work for

iterative pseudo-labeling. Therefore, instead of Eq. (13), we propose to use the entropy regularized OT problem, as defined in Eq. (14) below, which can be solved by the efficient Sinkhorn algorithm (Cuturi, 2013).

$$P^* = \arg \min_{P \in \Pi(\boldsymbol{\mu}, \boldsymbol{\nu})} \sum_{e_i \in \mathcal{E}'_1} \sum_{e_j \in \mathcal{E}'_2} P_{e_i, e_j} \cdot C_{e_i, e_j} + \beta \sum_{e_i \in \mathcal{E}'_1} \sum_{e_j \in \mathcal{E}'_2} P_{e_i, e_j} \log P_{e_i, e_j}, \quad (14)$$

where  $\beta$  is a hyper-parameter that controls the extent of regularization. Solving the above entropy regularized OT problem can be easily implemented using popular deep-learning frameworks like PyTorch and TensorFlow.

Once the optimal coupling matrix  $P^*$  is obtained, entity alignments can be inferred accordingly. Since one-to-one correspondences are crucial for eliminating conflicted misalignments (Type I pseudo-labeling errors), we propose a simple yet highly effective decision threshold to select entity pairs as pseudo-labels such that:

$$\hat{\mathcal{L}}_e = \{(e_i, e_j) \mid P_{e_i, e_j}^* > \frac{1}{2 \cdot \min(|\mathcal{E}'_1|, |\mathcal{E}'_2|)}, e_i \in \mathcal{E}'_1, e_j \in \mathcal{E}'_2\}. \quad (15)$$

This criterion ensures the pseudo-labels satisfy one-to-one correspondence with theoretical guarantee.

**Theorem 1.** *Any pseudo-labeled entity pair  $(e_i, e_j), e_i \in \mathcal{E}'_1, e_j \in \mathcal{E}'_2$  that satisfies the condition  $P_{e_i, e_j}^* > \frac{1}{2 \cdot \min(|\mathcal{E}'_1|, |\mathcal{E}'_2|)}$  warrants one-to-one correspondence such that no conflicted pairs  $\{(e_i, e_k) \mid e_k \in \mathcal{E}'_2 \setminus \{e_j\}\}$  and  $\{(e_l, e_j) \mid e_l \in \mathcal{E}'_1 \setminus \{e_i\}\}$  associated with  $e_i$  and  $e_j$ , respectively, are selected as pseudo-labels.*

*Proof.* Given a coupling matrix  $P^* \in \mathbb{R}_+^{|\mathcal{E}'_1| \times |\mathcal{E}'_2|}$  with the constraints of  $\sum_{e_j \in \mathcal{E}'_2} P_{e_i, e_j}^* = \frac{1}{|\mathcal{E}'_1|}$  for all rows ( $\forall e_i \in \mathcal{E}'_1$ ) and  $\sum_{e_i \in \mathcal{E}'_1} P_{e_i, e_j}^* = \frac{1}{|\mathcal{E}'_2|}$  for all columns ( $\forall e_j \in \mathcal{E}'_2$ ). Assume  $|\mathcal{E}'_1| < |\mathcal{E}'_2|$ , then the decision threshold is  $\frac{1}{2 \cdot \min(|\mathcal{E}'_1|, |\mathcal{E}'_2|)} = \frac{1}{2|\mathcal{E}'_1|}$ . Entity pairs  $\{(e_i, e_j) \mid P_{e_i, e_j}^* > \frac{1}{2|\mathcal{E}'_1|}, e_i \in \mathcal{E}'_1, e_j \in \mathcal{E}'_2\}$  are selected as pseudo-labels.

For each pseudo-labeled entity pair  $(e_i, e_j)$  with a probability value  $P_{e_i, e_j}^* > \frac{1}{2|\mathcal{E}'_1|}$ , we can prove that no conflicted pairs  $\{(e_i, e_k) \mid e_k \in \mathcal{E}'_2 \setminus \{e_j\}\}$  associated with  $e_i$  are selected as pseudo-labels:

$$\begin{aligned} P_{e_i, e_j}^* &> \frac{1}{2|\mathcal{E}'_1|}, \\ \sum_{e_j \in \mathcal{E}'_2} P_{e_i, e_j}^* - P_{e_i, e_j}^* &< \sum_{e_j \in \mathcal{E}'_2} P_{e_i, e_j}^* - \frac{1}{2|\mathcal{E}'_1|}, \\ \sum_{e_k \in \mathcal{E}'_2 \setminus \{e_j\}} P_{e_i, e_k}^* + P_{e_i, e_j}^* - P_{e_i, e_j}^* &< \frac{1}{|\mathcal{E}'_1|} - \frac{1}{2|\mathcal{E}'_1|}, \\ \sum_{e_k \in \mathcal{E}'_2 \setminus \{e_j\}} P_{e_i, e_k}^* &< \frac{1}{2|\mathcal{E}'_1|}. \end{aligned} \quad (16)$$

---

**Algorithm 1:** OT-based Pseudo-labeling with Sinkhorn Algorithm
 

---

**Input:** Two unaligned entity sets  $\mathcal{E}'_1 \subseteq \mathcal{E}_1$  and  $\mathcal{E}'_2 \subseteq \mathcal{E}_2$ . Transport cost matrix  $C$  and regularization hyper-parameter  $\beta$ .

**Output:** Pseudo-labeled entity pair set  $\hat{\mathcal{L}}_e$ .

- 1 Initialize  $P = \mathbf{1}_{|\mathcal{E}'_1|} \mathbf{1}_{|\mathcal{E}'_2|}^\top$ ;
- 2  $\mathbf{a} = \frac{1}{|\mathcal{E}'_1|} \mathbf{1}_{|\mathcal{E}'_1|}$ ,  $Z = e^{-\frac{1}{\beta}C}$ ;
- 3 **for** iteration in  $1 \dots k$  **do**
- 4      $Q = Z \odot P$ ;
- 5      $\mathbf{b} = \frac{1}{|\mathcal{E}'_1|Q^\top \mathbf{a}}$ ,  $\mathbf{a} = \frac{1}{|\mathcal{E}'_2|Q\mathbf{b}}$ ;
- 6      $P = \mathbf{a}\mathbf{b}^\top \odot Q$ ;
- 7 Obtain the optimal transport plan  $P^* = P$ ;
- 8 Obtain conflict-free pseudo-labels  
 $\hat{\mathcal{L}}_e = \{(e_i, e_j) \mid P_{e_i, e_j}^* > \frac{1}{2 \cdot \min(|\mathcal{E}'_1|, |\mathcal{E}'_2|)}, e_i \in \mathcal{E}'_1, e_j \in \mathcal{E}'_2\}$ ;
- 9 **return** pseudo-labeled entity pair set  $\hat{\mathcal{L}}_e$ .

---

Since the coupling matrix  $P^* \in \mathbb{R}_+^{|\mathcal{E}'_1| \times |\mathcal{E}'_2|}$  has non-negative entries, the summation  $\sum_{e_k \in \mathcal{E}'_2 \setminus \{e_j\}} P_{e_i, e_k}^*$  from Eq. (16) must be no smaller than any component of it, i.e.,  $P_{e_i, e_k}^* \leq \sum_{e_k \in \mathcal{E}'_2 \setminus \{e_j\}} P_{e_i, e_k}^*$ ,  $\forall e_k \in \mathcal{E}'_2 \setminus \{e_j\}$ . Together with Eq. (16), we can further derive that any component in the summation is smaller than the decision threshold, i.e.,  $P_{e_i, e_k}^* < \frac{1}{2|\mathcal{E}'_1|}$ ,  $\forall e_k \in \mathcal{E}'_2 \setminus \{e_j\}$ . In other words, all other probability values in the same row of  $P_{e_i, e_j}^*$  are smaller than the decision threshold. Thus, no conflicted pairs  $\{(e_i, e_k) \mid e_k \in \mathcal{E}'_2 \setminus \{e_j\}\}$  associated with  $e_i$  are selected.

Similarly, for each pseudo-labeled entity pair  $(e_i, e_j)$  with a probability value  $P_{e_i, e_j}^* > \frac{1}{2|\mathcal{E}'_1|}$ , we can prove that no conflicted pairs  $\{(e_l, e_j) \mid e_l \in \mathcal{E}'_1 \setminus \{e_i\}\}$  associated with entity  $e_j$  are selected as pseudo-labels. Similar to Eq. (16), we can also obtain  $\sum_{e_l \in \mathcal{E}'_1 \setminus \{e_i\}} P_{e_l, e_j}^* < \frac{1}{2|\mathcal{E}'_2|}$  and  $P_{e_l, e_j}^* \leq \sum_{e_l \in \mathcal{E}'_1 \setminus \{e_i\}} P_{e_l, e_j}^*$ ,  $\forall e_l \in \mathcal{E}'_1 \setminus \{e_i\}$ . Together with the assumption of  $|\mathcal{E}'_1| < |\mathcal{E}'_2|$ , we can further derive that  $P_{e_l, e_j}^* \leq \sum_{e_l \in \mathcal{E}'_1 \setminus \{e_i\}} P_{e_l, e_j}^* < \frac{1}{2|\mathcal{E}'_2|} < \frac{1}{2|\mathcal{E}'_1|}$ . Therefore, all other probability values in the same column of  $P_{e_i, e_j}^*$  are smaller than the decision threshold, i.e.,  $P_{e_l, e_j}^* < \frac{1}{2|\mathcal{E}'_1|}$ ,  $\forall e_l \in \mathcal{E}'_1 \setminus \{e_i\}$ . Hence, no conflicted pairs  $\{(e_l, e_j) \mid e_l \in \mathcal{E}'_1 \setminus \{e_i\}\}$  associated with entity  $e_j$  are selected.

In summary, we conclude that the selected pseudo-labels  $\{(e_i, e_j) \mid P_{e_i, e_j}^* > \frac{1}{2 \cdot \min(|\mathcal{E}'_1|, |\mathcal{E}'_2|)}, e_i \in \mathcal{E}'_1, e_j \in \mathcal{E}'_2\}$  are guaranteed to be one-to-one alignments when  $|\mathcal{E}'_1| < |\mathcal{E}'_2|$ , and the same conclusion also holds when  $|\mathcal{E}'_1| \geq |\mathcal{E}'_2|$ .  $\square$

The overall process of the OT-based pseudo-labeling algorithm is provided in Algorithm 1. In Steps 1-7, the Sinkhorn algorithm takes the transport cost matrix  $C$  as input to estimate the optimal transport plan  $P^*$  via  $k$  iterations of row normalization and column normalization. In Step 8, entity pairs with values in  $P^*$  larger than the decision threshold are selected as pseudo-labels. Finally, in Step 9, the model returns the set of pseudo-labeled entity pairs. The overall time complexity of Algorithm 1 is  $O(k \cdot |\mathcal{E}'_1| \cdot |\mathcal{E}'_2|)$ .

### 3.3 Cross-Iteration Pseudo-Label Calibration

Through OT-based pseudo-labeling, a set of conflict-free entity alignment pairs are obtained as pseudo-labels  $\hat{\mathcal{L}}_e^{(t)}$  at each iteration  $t$ . However, these pseudo-labels are still susceptible to one-to-one misalignments (Type II pseudo-labeling errors), especially at early training stages. Directly augmenting the prior alignment seeds with the pseudo-label set  $\hat{\mathcal{L}}_e^{(t)}$  would make the model overfit these errors, thereby deteriorating the confirmation bias. Therefore, we propose to further calibrate pseudo-labels through reducing the variability of pseudo-label selection across consecutive iterations. As such, the resultant pseudo-label set could have a higher precision and thus be more reliable.

Specifically, we obtain  $m$  sets of pseudo-labels  $\{\hat{\mathcal{L}}_e^{(t)} | t = 1, \dots, m\}$  respectively from every  $m$  consecutive iterations of pseudo-labeling. To prevent pseudo-labeling errors of previous iterations from adversely impacting the subsequent embedding learning, we randomly reinitialize model parameters during each of these  $m$  consecutive iterations, following the strategy proposed in (Cascante-Bonilla et al, 2021). This helps decorrelate the dependency among  $m$  consecutive iterations. Furthermore, inspired by ensemble learning (Yang et al, 2023), we propose to calibrate pseudo-labels by taking the common pseudo-labels among  $\{\hat{\mathcal{L}}_e^{(t)} | t = 1, \dots, m\}$ :

$$\cap_{t=1}^m \hat{\mathcal{L}}_e^{(t)} = \{(e_i, e_j) | \sum_{t=1}^m \mathbb{1}((e_i, e_j) \in \hat{\mathcal{L}}_e^{(t)}) = m, e_i \in \mathcal{E}'_1, e_j \in \mathcal{E}'_2\}, \quad (17)$$

where  $\mathbb{1}(\cdot)$  is a binary indicator function. By excluding pseudo-labels with high selection variability, we can effectively reduce the overall variability of pseudo-label selection to obtain calibrated pseudo-labels  $\cap_{t=1}^m \hat{\mathcal{L}}_e^{(t)}$ . Mathematically, we can prove that calibrated pseudo-labels have a higher precision than non-calibrated ones.

**Theorem 2.** *The alignment pseudo-labels generated via pseudo-label calibration over  $m$  consecutive iterations have a higher precision  $\mathbb{P}(y = 1 | \hat{y} = 1)$  than those generated at a single iteration, under the mild condition that  $\mathbb{P}(\hat{y} = 1 | (e_i, e_j), y = 1)$  is a constant  $p$  for each  $(e_i, e_j)$  at each iteration.*

*Proof.* At the  $t$ -th iteration, for an entity pair  $(e_i, e_j)$  with a ground-truth alignment label  $y = 0$ , the probability of aligning them is  $\mathbb{P}_t(\hat{y} = 1 | (e_i, e_j), y = 0)$ . With the pseudo-label calibration on  $m$  consecutive iterations, the alignment probability becomes  $\prod_{l=0}^{m-1} \mathbb{P}_{t+l}(\hat{y} = 1 | (e_i, e_j), y = 0)$ .

Similarly, at  $t$ -th iteration, for an entity pair  $(e_i, e_j)$  with ground-truth alignment label  $y = 1$ , the alignment probability is  $\mathbb{P}_t(\hat{y} = 1 | (e_i, e_j), y = 1) = p_t$ . With calibration, the alignment probability is  $\prod_{l=0}^{m-1} \mathbb{P}_{t+l}(\hat{y} = 1 | (e_i, e_j), y = 1) = \prod_{l=0}^{m-1} p_{t+l}$ . With the increase of iterations, we assume the alignment model is increasingly more accurate,

that is, we have

$$\begin{aligned} \prod_{l=0}^{m-1} \mathbb{P}_{t+l}(\hat{y} = 1 | (e_i, e_j), y = 0) &\leq \mathbb{P}_t^m(\hat{y} = 1 | (e_i, e_j), y = 0), \\ \prod_{l=0}^{m-1} \mathbb{P}_{t+l}(\hat{y} = 1 | (e_i, e_j), y = 1) &\geq \mathbb{P}_t^m(\hat{y} = 1 | (e_i, e_j), y = 1) = p_t^m. \end{aligned} \quad (18)$$

In the case with calibration, consider the probabilities,

$$\begin{aligned} \mathbb{P}_c(\hat{y} = 1, y = 0) &= \sum_{(e_i, e_j)} \prod_{l=0}^{m-1} \mathbb{P}_{t+l}(\hat{y} = 1 | (e_i, e_j), y = 0) \mathbb{P}((e_i, e_j), y = 0) \\ &\leq \sum_{(e_i, e_j)} \mathbb{P}_t^m(\hat{y} = 1 | (e_i, e_j), y = 0) \mathbb{P}((e_i, e_j), y = 0), \\ \mathbb{P}_c(\hat{y} = 1, y = 1) &= \sum_{(e_i, e_j)} \prod_{l=0}^{m-1} \mathbb{P}_{t+l}(\hat{y} = 1 | (e_i, e_j), y = 1) \mathbb{P}((e_i, e_j), y = 1) \\ &\geq \sum_{(e_i, e_j)} \mathbb{P}_t^m(\hat{y} = 1 | (e_i, e_j), y = 1) \mathbb{P}((e_i, e_j), y = 1), \\ \mathbb{P}_c(\hat{y} = 1, y = 1) &\geq \sum_{(e_i, e_j)} p_t^m \mathbb{P}((e_i, e_j), y = 1). \end{aligned} \quad (19)$$

Thus, we have

$$\frac{\mathbb{P}_c(\hat{y} = 1, y = 0)}{\mathbb{P}_c(\hat{y} = 1, y = 1)} \leq \frac{\sum_{(e_i, e_j)} \mathbb{P}_t^m(\hat{y} = 1 | (e_i, e_j), y = 0) \mathbb{P}((e_i, e_j), y = 0)}{\sum_{(e_i, e_j)} p_t^m \mathbb{P}((e_i, e_j), y = 1)}. \quad (20)$$

In the case without calibration, at the  $l$ -th iteration, we have

$$\frac{\mathbb{P}_t(\hat{y} = 1, y = 0)}{\mathbb{P}_t(\hat{y} = 1, y = 1)} = \frac{\sum_{(e_i, e_j)} \mathbb{P}_t(\hat{y} = 1 | (e_i, e_j), y = 0) \mathbb{P}((e_i, e_j), y = 0)}{\sum_{(e_i, e_j)} p_t \mathbb{P}((e_i, e_j), y = 1)}. \quad (21)$$

By comparing the two ratios,

$$\begin{aligned} \frac{\frac{\mathbb{P}_c(\hat{y}=1, y=0)}{\mathbb{P}_c(\hat{y}=1, y=1)}}{\frac{\mathbb{P}_t(\hat{y}=1, y=0)}{\mathbb{P}_t(\hat{y}=1, y=1)}} &\leq \frac{\frac{\sum_{(e_i, e_j)} \mathbb{P}_t^m(\hat{y}=1 | (e_i, e_j), y=0) \mathbb{P}((e_i, e_j), y=0)}{\sum_{(e_i, e_j)} p_t^m \mathbb{P}((e_i, e_j), y=1)}}{\frac{\sum_{(e_i, e_j)} \mathbb{P}_t(\hat{y}=1 | (e_i, e_j), y=0) \mathbb{P}((e_i, e_j), y=0)}{\sum_{(e_i, e_j)} p_t \mathbb{P}((e_i, e_j), y=1)}}, \\ \frac{\mathbb{P}_c(\hat{y}=1, y=0)}{\mathbb{P}_c(\hat{y}=1, y=1)} &\leq \frac{\sum_{(e_i, e_j)} \mathbb{P}_t^m(\hat{y} = 1 | (e_i, e_j), y = 0) \mathbb{P}((e_i, e_j), y = 0)}{\sum_{(e_i, e_j)} p_t^{m-1} \mathbb{P}_t(\hat{y} = 1 | (e_i, e_j), y = 0) \mathbb{P}((e_i, e_j), y = 0)}. \end{aligned} \quad (22)$$

**Lemma 1.** *If all pseudo-label sets  $\{\hat{\mathcal{L}}_e^{(t)} | t = 1, \dots, m\}$  have one-to-one correspondence and each pseudo-label set  $\hat{\mathcal{L}}_e^{(t)}$  has at least two correct alignments. Then the condition  $\mathbb{P}(\hat{y} = 1 | (e_i, e_j), y = 1) = p > \mathbb{P}(\hat{y} = 1 | (e_i, e_j), y = 0)$  holds.*

The detailed proof of Lemma 1 is provided in Appendix A. As  $\mathbb{P}_t(\hat{y} = 1 | (e_i, e_j), y = 0) < p_t = \mathbb{P}_t(\hat{y} = 1 | (e_i, e_j), y = 1)$ , then  $\mathbb{P}_t^m(\hat{y} = 1 | (e_i, e_j), y = 0) < p_t^{m-1} \mathbb{P}_t(\hat{y} = 1 | (e_i, e_j), y = 0)$  for each  $(e_i, e_j)$ . Therefore, we have

$$\frac{\frac{\mathbb{P}_c(\hat{y}=1, y=0)}{\mathbb{P}_c(\hat{y}=1, y=1)}}{\frac{\mathbb{P}_t(\hat{y}=1, y=0)}{\mathbb{P}_t(\hat{y}=1, y=1)}} < 1, \quad \text{i.e.,} \quad \frac{\mathbb{P}_c(\hat{y} = 1, y = 0)}{\mathbb{P}_c(\hat{y} = 1, y = 1)} < \frac{\mathbb{P}_t(\hat{y} = 1, y = 0)}{\mathbb{P}_t(\hat{y} = 1, y = 1)}. \quad (23)$$

Finally, the precision of pseudo-labels can be derived as:

$$\begin{aligned} \mathbb{P}(y = 1 | \hat{y} = 1) &= \frac{\mathbb{P}(\hat{y} = 1, y = 1)}{\mathbb{P}(\hat{y} = 1)} = \frac{\mathbb{P}(\hat{y} = 1, y = 1)}{\mathbb{P}(\hat{y} = 1, y = 0) + \mathbb{P}(\hat{y} = 1, y = 1)} \\ &= \frac{1}{\frac{\mathbb{P}(\hat{y}=1, y=0)}{\mathbb{P}(\hat{y}=1, y=1)} + 1}, \end{aligned} \quad (24)$$

whose value decreases with the increase of  $\frac{\mathbb{P}(\hat{y}=1, y=0)}{\mathbb{P}(\hat{y}=1, y=1)}$ . According to Eq. (23), we have

$$\mathbb{P}_c(y = 1 | \hat{y} = 1) > \mathbb{P}_t(y = 1 | \hat{y} = 1). \quad (25)$$

□

Theorem 2 implies that the precision of pseudo-labels increases after cross-iteration calibration, such that  $\mathbb{P}_c(y = 1 | \hat{y} = 1) > \mathbb{P}_t(y = 1 | \hat{y} = 1)$ , where  $\mathbb{P}_c$  and  $\mathbb{P}_t$  represent the probability of calibrated set, and the probability of non-calibrated set from iteration  $t$ , respectively.

Finally, the calibrated pseudo-labels are used to augment the prior alignment seeds:

$$\hat{\mathcal{L}}_e^0 \leftarrow \mathcal{L}_e^0 \cup \left( \bigcap_{t=1}^m \hat{\mathcal{L}}_e^{(t)} \right). \quad (26)$$

The augmented prior alignment seeds  $\hat{\mathcal{L}}_e^0$  contain a considerable number of reliably calibrated pseudo-labels with high precision for subsequent model training. This enables to effectively eliminate Type II pseudo-labeling errors and alleviate the problem of confirmation bias, thus boosting the performance of entity alignment in turn.

### 3.4 Overall Workflow

The overall procedure of the proposed UPL-EA model is described in Algorithm 2. In Step 1, the algorithm is initialized with the prior alignment seeds if provided. In Steps 3-8, the EA model and OT-based pseudo-labeling alternately reinforce each other towards learning more informative entity embeddings. During this process, negative alignment pairs are sampled in an adaptive manner for model training. In Steps 2-9, the pseudo-label calibration is performed every  $m$  iterations to augment the prior



---

**Algorithm 2:** Entity Alignment with UPL-EA Model

---

**Input:** Two knowledge graphs  $\mathcal{G}_1 = \{\mathcal{E}_1, \mathcal{R}_1, \mathcal{T}_1\}$ ,  $\mathcal{G}_2 = \{\mathcal{E}_2, \mathcal{R}_2, \mathcal{T}_2\}$ , prior alignment seeds  $\mathcal{L}_e^0$ .

**Output:** Inferred entity alignment pairs.

- 1 Initialize  $\hat{\mathcal{L}}_e^0 = \mathcal{L}_e^0$ ;
- 2 **repeat**
- 3     **for**  $t$  in  $1..m$  **do**
- 4         Obtain alignment pseudo-labels  $\hat{\mathcal{L}}_e^{(t)}$  with Algorithm 1;
- 5         Augment alignment seeds:  $\mathcal{L}_e \leftarrow \hat{\mathcal{L}}_e^0 \cup \hat{\mathcal{L}}_e^{(t)}$ ;
- 6         Sample negative pairs  $\mathcal{L}'_e$  according to  $\mathcal{L}_e$ ;
- 7         Learn entity embeddings with Eq. (6):  $\mathbf{h}_e \leftarrow \operatorname{argmin}_{\mathbf{h}_e} L$ ;
- 8         Augment prior alignment seeds with the calibrated pseudo-labels:  
           $\hat{\mathcal{L}}_e^0 \leftarrow \mathcal{L}_e^0 \cup (\cap_{t=1}^m \hat{\mathcal{L}}_e^{(t)})$ ;
- 9     **until** convergence or reaching a fixed number of epochs;
- 10 Use the final learned entity embeddings to infer new aligned entity pairs;
- 11 **return** *inferred entity alignment pairs*.

---

alignment seeds with reliably selected pseudo-labels for subsequent training. Finally, the learned entity embeddings are used to infer newly aligned entity pairs.

## 4 Experiments

In this section, we validate the efficacy of our proposed method through extensive experiments and ablation analyses on benchmark datasets.

### 4.1 Datasets and Baselines

We evaluate the performance of our UPL-EA<sup>1</sup> method on two benchmark datasets: DBP15K (Sun et al, 2017) and SRPRS (Guo et al, 2019). DBP15K is a widely used benchmark dataset for entity alignment (Ding et al, 2022; Liu et al, 2022; Wu et al, 2019a; Zhu et al, 2021). DBP15K contains three cross-lingual datasets, each of which contains two KGs built upon English and another different language (Chinese, Japanese or French). Each cross-lingual dataset has 15,000 aligned entity pairs. SRPRS is a more recently established benchmark dataset with sparser connections (Guo et al, 2019). SRPRS consists of two cross-lingual datasets, each having two KGs built upon English and French/German as well as 15,000 aligned entity pairs. The statistics of DBP15K and SRPRS are summarized in Table 1.

For evaluation, we compare UPL-EA with 12 state-of-the-art entity alignment models, which are categorized into two groups:

- Supervised models, including MTransE (Chen et al, 2017), JAPE (Sun et al, 2017), JAPE in its structure-only variant denoted as JAPE-Stru, GCN-Align (Wang et al, 2018), GCN-Align in its structure-only variant denoted as

---

<sup>1</sup>The source code of UPL-EA will be released publicly upon paper acceptance.

**Table 1:** Statistics of DBP15K and SRPRS datasets

Datasets		Entities	Relations	Rel.triplets
DBP15K <sub>ZH_EN</sub>	Chinese	66,469	2,830	153,929
	English	98,125	2,317	237,674
DBP15K <sub>JA_EN</sub>	Japanese	65,744	2,043	164,373
	English	95,680	2,096	233,319
DBP15K <sub>FR_EN</sub>	French	66,858	1,379	192,191
	English	105,889	2,209	278,590
SRPRS <sub>EN_FR</sub>	English	15,000	221	36,508
	French	15,000	177	33,532
SRPRS <sub>EN_DE</sub>	English	15,000	222	38,363
	German	15,000	120	37,377

GCN-Stru, RDGCN (Wu et al, 2019a), HGCN (Wu et al, 2019b), HMAN (Yang et al, 2019), and CEA (Zeng et al, 2020);

- Pseudo-labeling based models, including IPTransE (Zhu et al, 2017), BootEA (Sun et al, 2018), MRAEA (Mao et al, 2020), RNM (Zhu et al, 2021), and CPL-OT (Ding et al, 2022).

We utilize Hit@k ( $k = 1, 10$ ) and Mean Reciprocal Rank (MRR) as the evaluation metrics. Hit@k measures the percentage of correctly aligned entities ranked in the top k candidate list. MRR measures the average of the reciprocal ranks for the correctly aligned entities. Higher Hit@k and MRR scores indicate better entity alignment performance.

## 4.2 Experimental Setup

For fair comparisons, we follow the conventional 30%-70% ratio to randomly partition training and test data on DBP15K and SRPRS. We use semantic meanings of entity names to construct entity features. On DBP15K with big linguistic barriers, we first use Google Translate to translate non-English entity names into English, then look up 768-dimensional word embeddings pre-trained by BERT (Devlin et al, 2019) with English entity names to form entity features. On SRPRS with small linguistic barriers, we directly look up word embeddings without translation. As each entity name comprises one or multiple words, we further use TF-IDF to measure the contribution of each word towards entity name representation. Finally, we aggregate TF-IDF-weighted word embeddings for each entity to form its entity feature vector.

The parameter settings of UPL-EA is specified as follows:  $K = 125$ ,  $\beta = 0.5$ ,  $m = 3$ ,  $\gamma = 1$  and  $\lambda = 10$ . The embedding dimension  $d$  is set to 300. For BERT pre-trained word embeddings, we use a PCA-based technique (Raumak et al, 2019) to reduce feature dimension from 768 to 300 with minimal information loss. The batch size is set to 256 and the number of training epochs is set to 100. We implement our model in PyTorch. The Adam optimizer is used with a learning rate of 0.001 and 0.00025 on DBP15K and SRPRS, respectively. All experiments are run on a computer with an Intel(R) Core(TM) i9-13900KF CPU @ 3.00GHz and an NVIDIA Geforce RTX 4090 (24GB memory) GPU.

**Table 2:** Performance comparison on DBP15K

Models	DBP15K <sub>ZH_EN</sub>			DBP15K <sub>JA_EN</sub>			DBP15K <sub>FR_EN</sub>		
	Hit@1	Hit@10	MRR	Hit@1	Hit@10	MRR	Hit@1	Hit@10	MRR
MtransE	20.9	51.2	0.31	25.0	57.2	0.36	24.7	57.7	0.36
JAPE-Stru	37.2	68.9	0.48	32.9	63.8	0.43	29.3	61.7	0.40
GCN-Stru	39.8	72.0	0.51	40.0	72.9	0.51	38.9	74.9	0.51
JAPE*	41.4	74.1	0.53	36.5	69.5	0.48	31.8	66.8	0.44
GCN-Align*	43.4	76.2	0.55	42.7	76.2	0.54	41.1	77.2	0.53
HMAN*	56.1	85.9	0.67	55.7	86.0	0.67	55.0	87.6	0.66
RDGCN*	69.7	84.2	0.75	76.3	89.7	0.81	87.3	95.0	0.90
HGCN*	70.8	84.0	0.76	75.8	88.9	0.81	88.8	95.9	0.91
CEA*	78.7	-	-	86.3	-	-	97.2	-	-
IPTransE	33.2	64.5	0.43	29.0	59.5	0.39	24.5	56.8	0.35
BootEA	61.4	84.1	0.69	57.3	82.9	0.66	58.5	84.5	0.68
MRAEA	75.7	93.0	0.83	75.8	93.4	0.83	78.0	94.8	0.85
RNM*	84.0	91.9	0.87	87.2	94.4	0.90	93.8	98.1	0.95
CPL-OT*	<u>92.7</u>	<u>96.4</u>	<u>0.94</u>	<u>95.6</u>	<u>98.3</u>	<u>0.97</u>	<u>99.0</u>	<u>99.4</u>	<u>0.99</u>
UPL-EA	<b>94.9</b>	<b>97.4</b>	<b>0.96</b>	<b>97.0</b>	<b>98.8</b>	<b>0.98</b>	<b>99.5</b>	<b>99.7</b>	<b>1.00</b>

The results of MRAEA and CPL-OT on both benchmark datasets, and RNM on DBP15K are obtained from their original papers. Results of other baselines are obtained from (Zhao et al, 2020). For UPL-EA, we report the average results over five runs.

### 4.3 Comparison with State-of-the-Art Baselines

We compare the performance of the proposed UPL-EA with 12 state-of-the-art entity alignment baselines. Table 2 and Table 3 report performance comparisons on DBP15K and SRPRS, respectively. This set of results is reported with 30% prior alignment seeds used for training. The mark “\*” indicates that the semantic information of entity names is used to construct entity features. The best and second best results are highlighted in **boldface** and underlined, respectively.

Overall, UPL-EA significantly outperforms most of the existing EA models on five cross-lingual datasets. In particular, on DBP15K<sub>ZH\_EN</sub>, UPL-EA outperforms the second and third performers, CPL-OT and RNM, by over 2% and 10%, respectively, in terms of Hit@1. This affirms the necessity of systematically combating confirmation bias for pseudo-labeling-based entity alignment. It is worth noting that disparities in overall performance can be observed among the five cross-lingual datasets, where the lowest accuracy is achieved on DBP15K<sub>ZH\_EN</sub> due to its large linguistic barriers. Nevertheless, for the most challenging EA task on DBP15K<sub>ZH\_EN</sub>, UPL-EA yields strong performance gains over other baselines.

### 4.4 Comparison w.r.t. Different Rates of Prior Alignment Seeds

Table 4 further compares UPL-EA with four representative baselines (BootEA, RDGCN, RNM, and CPL-OT) with respect to different rates of prior alignment seeds

**Table 3:** Performance comparison on SRPRS

Models	SRPRS <sub>EN_FR</sub>			SRPRS <sub>EN_DE</sub>		
	Hit@1	Hit@10	MRR	Hit@1	Hit@10	MRR
MtransE	21.3	44.7	0.29	10.7	24.8	0.16
JAPE-Stru	24.1	53.3	0.34	30.2	57.8	0.40
GCN-Stru	24.3	52.2	0.34	38.5	60.0	0.46
JAPE*	24.1	54.4	0.34	26.8	54.7	0.36
GCN-Align*	29.6	59.2	0.40	42.8	66.2	0.51
HMAN*	40.0	70.5	0.50	52.8	77.8	0.62
RDGCN*	67.2	76.7	0.71	77.9	88.6	0.82
HGCN*	67.0	77.0	0.71	76.3	86.3	0.80
CEA*	96.2	-	-	97.1	-	-
IPTransE	12.4	30.1	0.18	13.5	31.6	0.20
BootEA	36.5	64.9	0.46	50.3	73.2	0.58
MRAEA	46.0	76.8	0.56	59.4	81.5	0.66
RNM*	92.5	96.2	0.94	94.4	96.7	0.95
CPL-OT*	97.4	98.8	0.98	97.4	98.9	0.98
UPL-EA	<b>98.2</b>	<b>99.3</b>	<b>0.99</b>	<b>98.4</b>	<b>99.5</b>	<b>0.99</b>

**Table 4:** Performance comparison w.r.t different rates of prior alignment seeds

Models	DBP15K <sub>ZH_EN</sub>				DBP15K <sub>JA_EN</sub>				DBP15K <sub>FR_EN</sub>			
	Hit@1											
	10%	20%	30%	40%	10%	20%	30%	40%	10%	20%	30%	40%
BootEA	45.7	57.3	62.9	67.9	42.9	53.5	62.2	66.0	47.3	59.8	65.3	68.6
RDGCN	66.6	68.9	70.8	72.6	72.4	74.5	76.7	79.0	86.3	87.6	88.6	89.7
RNM	79.3	81.7	84.0	85.4	83.4	85.9	87.2	88.8	92.3	93.0	93.8	94.5
CPL-OT	91.8	92.2	92.7	93.0	94.7	95.1	95.6	96.1	98.7	98.9	99.1	99.2
UPL-EA	<b>93.6</b>	<b>94.1</b>	<b>94.9</b>	<b>95.2</b>	<b>96.4</b>	<b>96.8</b>	<b>97.0</b>	<b>97.4</b>	<b>99.2</b>	<b>99.4</b>	<b>99.5</b>	<b>99.5</b>

varying from 10% to 40% on DBP15K. As expected, UPL-EA consistently outperforms four competitors on all three cross-lingual datasets at all rates. This is attributed to UPL-EA’s ability to augment the training set with reliable pseudo-labeled entity pairs by effectively alleviating confirmation bias. As the rate of prior alignment seeds decreases, the performance of BootEA significantly degrades due to its limited ability to prevent the accumulation of pseudo-labeling errors. RNM yields performance gains over RDGCN owing to its posterior embedding distance editing using iteratively pseudo-labeled entity pairs; however, the lack of iterative model re-training largely hinders its performance. CPL-OT demonstrates more stable performance with different rates of prior alignment seeds because it selects pseudo-labels via the conflict-aware OT modeling and then uses them to train entity alignment model in turn; nevertheless, the neglect of one-to-one misalignments (Type II pseudo-labeling errors) limits the potential of CPL-OT. In contrast, the performance of UPL-EA remains competitively stable when the rate of prior alignment seeds decreases, even on the most challenging DBP15K<sub>ZH\_EN</sub> dataset.

**Table 5:** Ablation study on DBP15K

Models	DBP15K <sub>ZH_EN</sub>			DBP15K <sub>JA_EN</sub>			DBP15K <sub>FR_EN</sub>		
	Hit@1	Hit@10	MRR	Hit@1	Hit@10	MRR	Hit@1	Hit@10	MRR
30% Prior Alignment Seeds									
Full Model	<b>94.9</b>	<b>97.4</b>	<b>0.96</b>	<b>97.0</b>	<b>98.8</b>	<b>0.98</b>	<b>99.5</b>	<b>99.7</b>	<b>1.00</b>
w.o. Global-lev. Rel. Aggr.	92.6	96.4	0.94	96.4	98.5	0.97	99.3	99.7	1.00
w.o. Within-iter. OT	80.1	90.4	0.84	87.6	94.8	0.90	94.4	97.4	0.96
w.o. Cross-iter. Calibration	84.9	90.6	0.87	91.1	95.5	0.93	98.1	99.0	0.98
w.o. Within & Cross-iter.	74.8	87.3	0.80	83.4	93.6	0.87	93.1	97.5	0.95
No Prior Alignment Seeds									
Full Model	<b>93.1</b>	<b>96.2</b>	<b>0.94</b>	<b>95.7</b>	<b>98.3</b>	<b>0.97</b>	<b>99.2</b>	<b>99.5</b>	<b>0.99</b>
w.o. Global-lev. Rel. Aggr.	91.4	95.3	0.93	95.3	98.1	0.96	99.1	99.7	0.99
w.o. Within-iter. OT	66.9	75.5	0.70	76.9	85.2	0.80	91.9	95.2	0.93
w.o. Cross-iter. Calibration	83.0	88.7	0.85	90.1	94.6	0.92	97.8	98.8	0.98
w.o. Within & Cross-iter.	67.1	76.8	0.71	77.1	86.2	0.81	91.4	95.9	0.93

**Table 6:** Ablation study on SRPRS

Models	SRPRS <sub>EN_FR</sub>			SRPRS <sub>EN_DE</sub>		
	Hit@1	Hit@10	MRR	Hit@1	Hit@10	MRR
30% Prior Alignment Seeds						
Full Model	<b>98.2</b>	<b>99.3</b>	<b>0.99</b>	<b>98.4</b>	<b>99.5</b>	<b>0.99</b>
w.o. Global-lev. Rel. Aggr.	97.5	98.9	0.98	97.8	99.2	0.98
w.o. Within-iter. OT	93.9	96.6	0.95	94.2	97.5	0.95
w.o. Cross-iter. Calibration	94.6	97.4	0.96	94.8	98.1	0.96
w.o. Within & Cross-iter.	92.7	96.5	0.94	93.6	97.4	0.95
No Prior Alignment Seeds						
Full Model	<b>97.9</b>	<b>99.2</b>	<b>0.98</b>	<b>97.7</b>	<b>99.2</b>	<b>0.98</b>
w.o. Global-lev. Rel. Aggr.	97.1	98.6	0.98	97.4	98.7	0.98
w.o. Within-iter. OT	89.8	93.0	0.91	91.4	95.2	0.93
w.o. Cross-iter. Calibration	94.2	97.0	0.95	94.8	97.7	0.96
w.o. Within & Cross-iter.	89.7	93.1	0.91	91.1	94.9	0.93

## 4.5 Ablation Study

To testify the importance of different key components of the proposed UPL-EA model, we conduct a series of ablation studies on five cross-lingual datasets from DBP15K and SRPRS. To provide more insights, apart from the conventional setting using 30% prior alignment seeds as training data, we also conduct our analysis on the setting with no prior alignment seeds. The full UPL-EA model is compared with its ablated variants, with the best performance highlighted by **boldface**. From Table 5 and Table 6, we can see that the full UPL-EA model performs best in all cases.

- **w.o. Global-lev. Rel. Aggr.:** We compare the full UPL-EA model against the variant without using global-level relation aggregation for entity embedding learning. This ablation leads to degraded performance on both settings primarily due to the increase in conflicted misalignments caused by feature over-smoothing.

- **w.o. Within-iter. OT:** To study the effectiveness of within-iteration OT modeling for pseudo-labeling, we ablate it from the full UPL-EA model. As OT modeling can eliminate a considerable number of conflicted misalignments (Type I pseudo-labeling errors) to ensure one-to-one alignments at each iteration, this ablation results in a significant performance drop across all datasets in both settings.
- **w.o. Cross-iter. Calibration:** To study the efficacy of cross-iteration pseudo-label calibration, we remove it from UPL-EA. This ablation has a profound negative effect, leading to substantial performance declines in both settings, especially on DBP15K<sub>ZH\_EN</sub> and DBP15K<sub>JA\_EN</sub> with large linguistic barriers, whereas the performance drops are smaller on DBP15K<sub>FR\_EN</sub> with relatively small linguistic barriers. This is because larger linguistic barriers tend to incur more one-to-one misalignments (Type II pseudo-labeling errors). Our findings confirm that pseudo-label calibration is crucial for UPL-EA to achieve its full potential, especially when there exists a large number of pseudo-labeling errors at the beginning of model training.
- **w.o. Within & Cross-iter.:** We also analyze the overall effect of ablating both within-iteration OT modeling and cross-iteration pseudo-label calibration from the full model. This ablation has a substantial adverse impact, leading to a dramatic performance drop in all cases. The results demonstrate the effectiveness of our unified UPL-EA framework in systematically combating confirmation bias for pseudo-labeling-based entity alignment.

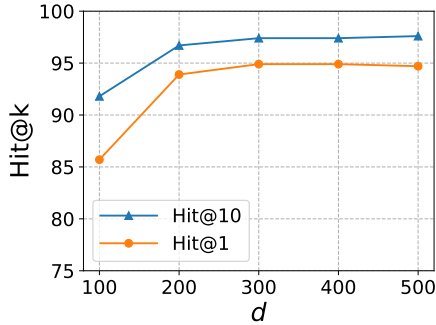
Note that under the setting with no prior alignment seeds, the variant without OT-based pseudo-labeling (w.o. Within-iter. OT) has similar performance as compared to the variant completely ignoring confirmation bias (w.o. Within & Cross-iter.). In particular, on DBP15K<sub>ZH\_EN</sub> and DBP15K<sub>JA\_EN</sub>, the former variant even performs slightly worse. This is because under the challenging case where there are no prior alignment seeds, ablating OT-based pseudo-labeling might incur considerably more conflicted misalignments (Type I pseudo-labeling errors), violating Lemma 1 and thus making Theorem 2 invalid because the number of misalignments (false positives) is not bounded. As a result, it becomes ineffective to calibrate erroneous pseudo-labels.

## 4.6 Impact of Pre-trained Word Embeddings

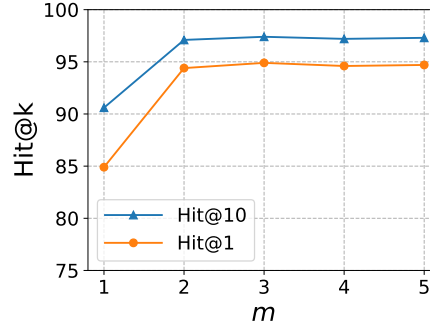
To analyze the impact of using different pre-trained word embeddings, we report the results of UPL-EA that form entity features with Glove embedding (Pennington et al, 2014), which is widely used in the existing EA models. We conduct this analysis on the setting with 30% prior alignment seeds. The results on DBP15K are reported in Table 7 as a case study. We can observe that UPL-EA with Glove embedding still achieves competitive results, significantly outperforming all other baselines. This confirms that the efficacy of UPL-EA is not highly dependent on embedding initialization methods used. When switching from Glove embedding to BERT pre-trained embeddings, performance gains can be observed, especially on DBP15K<sub>JA\_EN</sub>. This indicates the usefulness of pre-trained word embeddings with high quality for entity alignment.

**Table 7:** Impact of pre-trained word embeddings

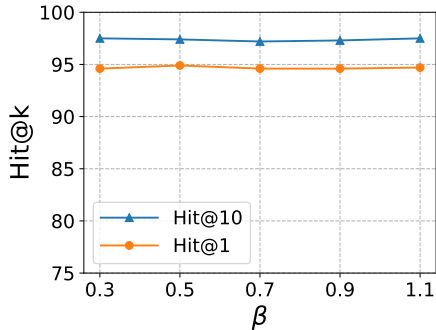
Models	DBP15K <sub>ZH_EN</sub>			DBP15K <sub>JA_EN</sub>			DBP15K <sub>FR_EN</sub>		
	Hit@1	Hit@10	MRR	Hit@1	Hit@10	MRR	Hit@1	Hit@10	MRR
Glove	94.0	97.6	0.95	95.9	98.9	0.97	99.1	99.8	0.99
BERT	94.9	97.4	0.96	97.0	98.8	0.98	99.5	99.7	1.00



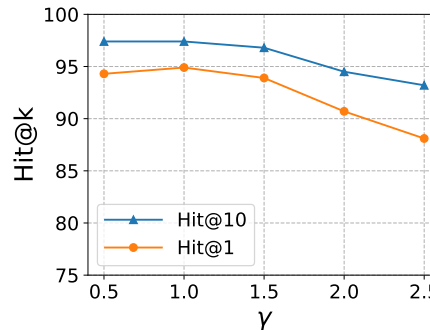
(a) Embedding dimension  $d$



(b) Number of iterations for calibration  $m$



(c) Regularization hyper-parameter  $\beta$



(d) Margin hyper-parameter  $\gamma$

**Fig. 4:** Hyper-parameter sensitivity study on DBP15K<sub>ZH\_EN</sub>

## 4.7 Parameter Sensitivity Study

We further study the sensitivity of our UPL-EA model with regards to four hyper-parameters: embedding dimension  $d$ , number of iterations  $m$  for cross-iteration pseudo-label calibration, regularization hyper-parameter  $\beta$  for Sinkhorn algorithm, and margin parameter  $\gamma$  for defining the alignment ranking loss. This sensitivity analysis is conducted on DBP15K<sub>ZH\_EN</sub> with 30% prior alignment seeds as a case study. The respective results in terms of Hit@1 and Hit@10 are plotted in Fig. 4.

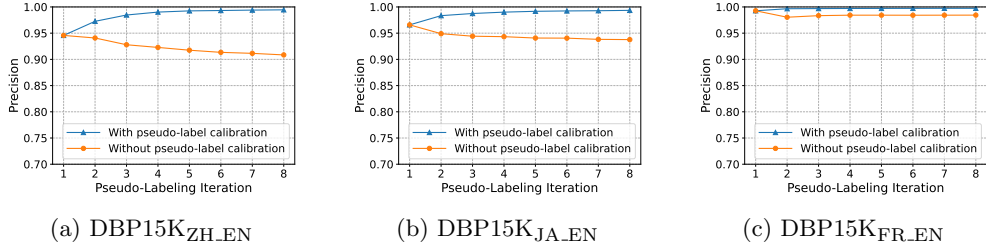


**Fig. 5:** Precision comparison between pseudo-labeling with calibration and without calibration

As we can see from Fig. 4a, the performance of UPL-EA improves considerably as the embedding dimension  $d$  increases from 100 to 300 and then retains at a relatively stable level. For the number of iterations  $m$  used for pseudo-label calibration, having cross-iteration calibration ( $m > 1$ ) leads to considerably better performance as opposed to not having calibration ( $m = 1$ ). This proves the effectiveness of our proposed calibration mechanism, requiring only a very small number of iterations used for calibration (i.e.,  $m = 3$ ) to achieve competitive performance (see Fig. 4b). In addition, as observed in Fig. 4c, the performance of UPL-EA is insensitive to different values of  $\beta$  associated with OT-based pseudo-labeling. As for the margin parameter  $\gamma$ , the performance of UPL-EA starts to drop gradually after  $\gamma$  exceeds 1, as shown in Fig. 4d. This observation is reasonable, as a larger margin parameter would give more tolerance to alignment errors, thus degrading model performance.

#### 4.8 Empirical Evidence on the Effectiveness of Pseudo-label Calibration

Lastly, to validate the effectiveness of cross-iteration pseudo-label calibration, we perform an empirical analysis to compare the precision of pseudo-labeling with and without calibration. This empirical analysis is carried out on DBP15K as a case study and under the setting with 30% prior alignment seeds. In Fig. 5, we directly compare the precision between pseudo-labeling with calibration (indicated by the blue curve) and without calibration (indicated by the orange curve) over eight pseudo-labeling iterations. Notably, pseudo-labeling with calibration consistently achieves a higher precision compared to pseudo-labeling without calibration throughout the training process. This discrepancy is particularly profound in the case of DBP15K<sub>ZH\_EN</sub> and DBP15K<sub>JA\_EN</sub>, where significant linguistic barriers exist. Specifically, without calibration, the precision of pseudo-labeling deteriorates gradually as the training progresses due to confirmation bias arising from the accumulation of one-to-one misalignments (Type II pseudo-labeling errors). In contrast, when employing pseudo-label calibration, the precision of pseudo-labeling approaches to almost 100% after only three consecutive iterations across all datasets. These findings affirm the necessity and efficacy of calibrating pseudo-labels across iterations to mitigate the adverse impact of confirmation bias, particularly on challenging datasets like DBP15K<sub>ZH\_EN</sub>.



## 5 Related Work

In this section, we review three streams of related literature, including entity alignment in knowledge graphs, pseudo-labeling in semi-supervised learning, and optimal transport on graphs.

### 5.1 Entity Alignment in Knowledge Graphs

Most entity alignment models are embedding-based approaches, which exploit distances between entity embeddings in latent spaces to measure inherent semantic correspondences between entities. Inspired by TransE (Bordes et al, 2013), MTransE (Chen et al, 2017) embeds two KGs into two respective embedding spaces, where a transformation matrix is learned using prior alignment seeds. To reduce the number of parameters involved, most subsequent models (Sun et al, 2017, 2018; Zhu et al, 2017) embed KGs into a common latent space by imposing the embeddings of pre-aligned entities to be as close as possible. This ensures that alignment similarities between entities can be directly measured via their embeddings.

To leverage KG structural information, methods like GCN-Align (Wang et al, 2018) utilize GCNs to obtain better embeddings for entity alignment. However, GCNs and their variants are inclined to result in alignment conflicts, as their feature smoothness scheme tends to make entities have similar embeddings among local neighborhoods. To reduce the over-smoothing effect, more recent works (Wu et al, 2019b,a; Zhu et al, 2021) adopt a highway strategy (Srivastava et al, 2015) on GCN layers, which “mixes” the learned entity embeddings with the original features. Another line of research efforts is devoted to improving GCN-based approaches through considering heterogeneous relations in KGs. HGCN (Wu et al, 2019b) jointly learns the embeddings of entities and relations, without considering the directions of relations. RDGCN (Wu et al, 2019a) performs embedding learning on a dual relation graph, but fails to incorporate statistical information of neighboring relations of an entity. RNM (Zhu et al, 2021) uses iterative relational neighborhood matching to refine finalized entity embedding distances. This matching mechanism proves to be empirically effective, but it is used only after the completion of model training and fails to reinforce embedding learning in turn. All the aforementioned models, however, require an abundance of prior alignment seeds provided for training purposes, which are labor-intensive and costly to acquire in real-world KGs.

To tackle the shortage of prior alignment seeds, semi-supervised EA models have been proposed in recent years. As a prominent learning paradigm among such, pseudo-labeling-based methods, e.g., BootEA (Sun et al, 2018), IPTransE (Zhu et al, 2017), RNM (Zhu et al, 2021), MRAEA (Mao et al, 2020), and CPL-OT (Ding et al, 2022), propose to iteratively pseudo-label unaligned entity pairs and add them to prior alignment seeds for subsequent model retraining. For RNM, there is a slight difference that it augments prior alignment seeds to rectify embedding distance after the completion of model training. Although these methods have achieved promising performance gains, the confirmation bias associated with iterative pseudo-labeling has been largely under-explored. Only limited attempts have been recently made to alleviate Type I pseudo-labeling errors (conflicted misalignments) while Type II errors (one-to-one

misalignments) have been completely overlooked. To eliminate Type I pseudo-labeling errors, RNM (Zhu et al, 2021) and MRAEA (Mao et al, 2020) use simple heuristics to preserve only the most convincing alignment pairs, for example, those with the smallest distance, at the presence of conflicts. BootEA (Sun et al, 2018) and CPL-OT (Ding et al, 2022), on the other hand, model the inference of pseudo-labeled entity pairs as an assignment problem, where the most likely aligned pairs are selected at each pseudo-labeling iteration. Unlike BootEA that selects a small set of pseudo-labels using a pre-specified threshold, CPL-OT imposes a full match between two unaligned entity sets to maximize the number of pseudo-labels at each iteration. Nevertheless, both methods impose constraints to enforce hard alignments for the purpose of alleviating alignment conflicts, but this might potentially lead to an increase in more one-to-one misalignments (Type II errors).

To fill in the research gap, our work explicitly tackles both Type I and Type II pseudo-labeling errors to combat confirmation bias in a principled way. The proposed UPL-EA effectively eliminates Type I pseudo-labeling errors by casting entity alignment inference into a discrete OT problem; this formulation enables more accurate determination of entity correspondences across KGs. In combination with a carefully designed selection criterion, UPL-EA is guaranteed to generate one-to-one alignments as pseudo-labels at each iteration. Furthermore, UPL-EA calibrates pseudo-labels by reducing local pseudo-label selection variability across iterations to alleviate Type II pseudo-labeling errors, preventing erroneous pseudo-labels from propagating and jeopardizing subsequent model training.

## 5.2 Pseudo-Labeling

Pseudo-labeling has emerged as an effective semi-supervised approach in addressing the challenge of label scarcity. It refers to a self-training paradigm where the model is iteratively bootstrapped with additional labeled data based on its own predictions. The pseudo-labels generated from model predictions can be defined as hard (one-hot distribution) or soft (continuous distribution) labels (Lee, 2013; Shi et al, 2018; Arazo et al, 2020). More specifically, pseudo-labeling strategies are designed to select high-confidence unlabeled data by either directly taking the model’s predictions, or sharpening the predicted probability distribution. It is closely related to entropy regularization (Sajjadi et al, 2016), where the model’s predictions are encouraged to have low entropy (i.e., high-confidence) on unlabeled data. The selected pseudo-labels are then used to augment the training set and to fine-tune the model initially trained on the given labels. This training regime is also extended to an explicit teacher-student configuration (Pham et al, 2021), where a teacher network generates pseudo-labels from unlabeled data, which are used to train a student network.

Despite its promising results, pseudo-labeling is inevitably susceptible to erroneous pseudo-labels, thus suffering from confirmation bias (Arazo et al, 2020; Rizve et al, 2021), where the prediction errors would accumulate and degrade model performance. The confirmation bias has been recently studied in the field of computer vision. In works like (Arazo et al, 2020; Rizve et al, 2021), confirmation bias is considered as a problem of poor network calibration, where the network is overfitted towards erroneous pseudo-labels. To alleviate confirmation bias, pseudo-labeling approaches have

adopted strategies such as mixup augmentation (Arazo et al, 2020) and uncertainty weighting (Rizve et al, 2021). Subsequent works like (Cascante-Bonilla et al, 2021; Zhang et al, 2021) address confirmation bias by applying curriculum learning principles, where the decision threshold is adaptively adjusted during the training process and model parameters are re-initialized after each iteration.

Recently, pseudo-labeling has also been studied on graphs for the task of semi-supervised node classification (Li et al, 2018; Sun et al, 2020; Li et al, 2023). Li et al (2018) propose a self-trained GCN that enlarges the training set by assigning a pseudo-label to high-confidence unlabeled nodes, and then re-trains the model using both genuine labels and pseudo-labels. The pseudo-labels are generated via a random walk model in a co-training manner. Sun et al (2020) show that a shallow GCN is ineffective in propagating label information under few-label settings, and employ a multi-stage self-training approach that relies on a deep clustering model to assign pseudo-labels. Li et al (2023) propose to incorporate the node informativeness scores for the selection of pseudo-labels and adopt distinct loss functions for genuine labels and pseudo-labels during model training. Despite these research efforts, the problem of confirmation bias remains under-explored in graph domains. This work systematically analyzes the cause of confirmation bias and proposes a principled approach to conquer confirmation bias for pseudo-labeling-based entity alignment across KGs.

### 5.3 Optimal Transport on Graphs

Optimal Transport (OT) is the general problem of finding an optimal plan to move one distribution of mass to another with the minimal cost (Villani, 2009). As an effective metric to define the distance between probability distributions, OT has been applied in computer vision and natural language processing over a range of tasks including machine translation, text summarization, and image captioning (Torres et al, 2021; Chen et al, 2020). In recent years, OT has also been studied on graphs to match graphs with similar structures or align nodes/entities across graphs. For graph partitioning and matching, the transport on the edges across graphs has been used to define the Gromov-Wasserstein (GW) discrepancy (Titouan et al, 2019) that measures how the edges in a graph compare to those in another graph (Xu et al, 2019b; Maretic et al, 2019; Xu et al, 2019a). For entity alignment across graphs, Pei et al (2019) incorporate an OT objective into the overall loss to enhance the learning of entity embeddings. Tang et al (2023) propose to jointly perform structure learning and OT alignment through minimizing the multi-view GW distance matrices between two attributed graphs. These methods have primarily used OT to define a learning objective, which involves bi-level optimization for model training. To further enhance the scalability of OT modeling for entity alignment, Mao et al (2022) propose to make the similarity matrix sparse by dropping its entries close to zero. However, this sparse OT modeling potentially violates the constraints of the OT objective, thereby failing to guarantee one-to-one correspondences across two KGs. In our work, we focus on tackling the scarcity of prior alignment seeds via iterative pseudo-labeling; we seek to find more accurate correspondences between entities via OT modeling. This enables

us to derive a one-to-one alignment configuration more precisely to eliminate conflicted misalignments (Type I pseudo-labeling errors) at each iteration, mitigating the negative impact of confirmation bias.

## 6 Conclusion

We proposed a novel unified pseudo-labeling framework (UPL-EA) that addresses the problem of confirmation bias for pseudo-labeling-based entity alignment across KGs. UPL-EA employs an entity alignment model based on the global-local aggregation architecture to generate informative entity embeddings. In addition, UPL-EA includes two modules to combat confirmation bias: within-iteration Optimal Transport (OT)-based pseudo-labeling and cross-iteration pseudo-label calibration. The OT-based pseudo-labeling module utilizes OT modeling to eliminate conflicted misalignments (Type I pseudo-labeling errors) within each iteration. The pseudo-label calibration module employs pseudo-labels from multiple consecutive iterations to reduce pseudo-label selection variability, thus preventing the accumulation and propagation of inevitable one-to-one misalignments (Type II pseudo-labeling errors) across iterations. Our extensive experiments on benchmark datasets show that UPL-EA outperforms state-of-the-art baselines with limited amounts of prior alignment seeds. The competitive performance of UPL-EA demonstrates its superiority in addressing confirmation bias and its potential for pseudo-labeling-based entity alignment across KGs.

## Appendix A Proof of Lemma 1

*Proof.* Given two unaligned entity sets  $\mathcal{E}'_1 \in \mathcal{G}_1$  and  $\mathcal{E}'_2 \in \mathcal{G}_2$ , there is an entity alignment candidate space  $\mathcal{E}'_1 \times \mathcal{E}'_2 \in \{y = 0, y = 1\}^{|\mathcal{E}'_1| \times |\mathcal{E}'_2|}$ . The pseudo-label selection process can be considered as a classification problem, where each entity pair  $(e_i, e_j)$ ,  $e_i \in \mathcal{E}'_1$ ,  $e_j \in \mathcal{E}'_2$  in the candidate space is classified as either being aligned ( $\hat{y} = 1$ ) or not aligned ( $\hat{y} = 0$ ). Let  $|\mathcal{E}'_1| = m$  and  $|\mathcal{E}'_2| = n$ , we can thus obtain a confusion matrix based on the pseudo-label selection with one-to-one correspondence as given in Table A1.

**Table A1:** Confusion matrix for entity alignment classification via pseudo-label selection with one-to-one correspondence

	$y = 1$	$y = 0$	Sum
$\hat{y} = 1$	$TP$	$FP$	$0 \leq TP + FP \leq \min(m, n)$
$\hat{y} = 0$	$FN$	$TN$	$mn \geq FN + TN \geq mn - \min(m, n)$
Sum	$= \min(m, n)$	$= mn - \min(m, n)$	$TP + FP + FN + TN = mn$

$TP$ ,  $FP$ ,  $FN$  and  $TN$  represent “True Positive”, “False Positive”, “False Negative” and “True Negative”, respectively. The number of ground truth entity alignment pairs

with  $y = 1$  is  $TP + FN = \min(m, n)$ . Correspondingly, the number of ground truth entity pairs that are not aligned ( $y = 0$ ) is  $FP + TN = mn - \min(m, n)$ . Since the pseudo-labels obtained using our proposed OT-based modeling satisfy one-to-one correspondence, the number of pseudo-labeled entity pairs with  $\hat{y} = 1$  is bounded, i.e.,  $0 \leq TP + FP \leq \min(m, n)$ , thus the number of misalignments is bounded such that  $FP \leq \min(m, n) - TP$ .

Denote  $p = \mathbb{P}(\hat{y} = 1 | (e_i, e_j), y = 1)$  and  $p' = \mathbb{P}(\hat{y} = 1 | (e_i, e_j), y = 0)$ . Let us consider two cases below.

- When  $m < n$ , we have  $\min(m, n) = m$ ,  $FP \leq m - TP$ ,  $0 < \frac{m}{n} < 1$ . Thus,

$$p = \frac{TP}{TP + FN} = \frac{TP}{m}, \quad p' = \frac{FP}{FP + TN} = \frac{FP}{mn - m}. \quad (\text{A1})$$

We can calculate the ratio

$$\frac{p}{p'} = \frac{TP}{m} \cdot \frac{mn - m}{FP} = \frac{TP}{FP} \cdot (n - 1). \quad (\text{A2})$$

For the condition  $p > p'$  to hold, we have

$$\begin{aligned} \frac{p}{p'} &= \frac{TP}{FP}(n - 1) > 1, \\ TP(n - 1) &> FP, \end{aligned} \quad (\text{A3})$$

Since  $FP \leq m - TP$ , we ensure

$$\begin{aligned} TP(n - 1) &> m - TP, \\ nTP - TP &> m - TP, \\ TP &> \frac{m}{n}, \end{aligned} \quad (\text{A4})$$

Since  $0 < \frac{m}{n} < 1$ , we ensure  $TP \geq 1$ . Therefore, as long as there is at least one correct alignment ( $TP \geq 1$ ) in the pseudo-label set when  $m < n$ , the condition  $p > p'$  holds.

- Similarly, when  $m \geq n$ ,  $\min(m, n) = n$ , we have  $FP \leq n - TP$ ,  $0 < \frac{n}{m} \leq 1$ . Thus,

$$p = \frac{TP}{n}, \quad p' = \frac{FP}{mn - n}, \quad \frac{p}{p'} = \frac{TP}{FP} \cdot (m - 1). \quad (\text{A5})$$

For the condition  $p > p'$  to hold, we have

$$\begin{aligned} \frac{p}{p'} &= \frac{TP}{FP}(m - 1) > 1, \\ TP(m - 1) &> FP, \end{aligned} \quad (\text{A6})$$

Since  $FP \leq n - TP$ , we ensure

$$\begin{aligned} mTP - TP &> n - TP, \\ TP &> \frac{n}{m}, \end{aligned} \tag{A7}$$

Since  $0 < \frac{n}{m} \leq 1$ , we ensure  $TP > 1$ . Therefore, as long as there are at least two correct alignments ( $TP \geq 2 > 1$ ) in the pseudo-label set when  $m \geq n$ , the condition  $p > p'$  holds.

Putting together, as long as there are at least two correct alignments ( $TP \geq 2$ ) in the pseudo-label set with one-to-one correspondence, the condition  $\mathbb{P}(\hat{y} = 1 | (e_i, e_j), y = 1) = p > \mathbb{P}(\hat{y} = 1 | (e_i, e_j), y = 0)$  holds.  $\square$

## References

- Arazo E, Ortego D, Albert P, et al (2020) Pseudo-labeling and confirmation bias in deep semi-supervised learning. In: IJCNN, IEEE, pp 1–8
- Bollacker K, Evans C, Paritosh P, et al (2008) Freebase: a collaboratively created graph database for structuring human knowledge. In: SIGMOD, pp 1247–1250
- Bordes A, Usunier N, Garcia-Durán A, et al (2013) Translating embeddings for modeling multi-relational data. In: NeurIPS, pp 2787–2795
- Cascante-Bonilla P, Tan F, Qi Y, et al (2021) Curriculum labeling: Revisiting pseudo-labeling for semi-supervised learning. In: AAAI, pp 6912–6920
- Chen L, Gan Z, Cheng Y, et al (2020) Graph optimal transport for cross-domain alignment. In: ICML, pp 1542–1553
- Chen M, Tian Y, Yang M, et al (2017) Multilingual knowledge graph embeddings for cross-lingual knowledge alignment. In: IJCAI, pp 1511–1517
- Cuturi M (2013) Sinkhorn distances: Lightspeed computation of optimal transport. In: NeurIPS, pp 2292–2300
- Devlin J, Chang M, Lee K, et al (2019) BERT: pre-training of deep bidirectional transformers for language understanding. In: NAACL-HLT, ACL, pp 4171–4186
- Ding Q, Zhang D, Yin J (2022) Conflict-aware pseudo labeling via optimal transport for entity alignment. In: ICDM, IEEE, pp 915–920
- Guo L, Sun Z, Hu W (2019) Learning to exploit long-term relational dependencies in knowledge graphs. In: ICML, pp 2505–2514
- Guo Q, Zhuang F, Qin C, et al (2022) A survey on knowledge graph-based recommender systems. IEEE Transactions on Knowledge and Data Engineering 34(8):3549–3568

- Kipf TN, Welling M (2017) Semi-supervised classification with graph convolutional networks. In: ICLR
- Lee DH (2013) Pseudo-label: The simple and efficient semi-supervised learning method for deep neural networks. In: ICML Workshop: Challenges in Representation Learning, p 896
- Li Q, Han Z, Wu X (2018) Deeper insights into graph convolutional networks for semi-supervised learning. In: AAAI, pp 3538–3545
- Li Y, Yin J, Chen L (2023) Informative pseudo-labeling for graph neural networks with few labels. *Data Mining and Knowledge Discovery* 37:228—254
- Liu X, Hong H, Wang X, et al (2022) Selfkg: Self-supervised entity alignment in knowledge graphs. In: WWW, pp 860–870
- Mao X, Wang W, Xu H, et al (2020) Mraea: an efficient and robust entity alignment approach for cross-lingual knowledge graph. In: WSDM, pp 420–428
- Mao X, Wang W, Wu Y, et al (2022) Lightea: A scalable, robust, and interpretable entity alignment framework via three-view label propagation. In: EMNLP, pp 825–838
- Maretic HP, Gheche ME, Chierchia G, et al (2019) GOT: an optimal transport framework for graph comparison. In: NeurIPS, pp 13876–13887
- Orlin JB (1997) A polynomial time primal network simplex algorithm for minimum cost flows. *Mathematical Programming* 78:109–129
- Paulheim H (2017) Knowledge graph refinement: A survey of approaches and evaluation methods. *Semantic Web* 8(3):489–508
- Pei S, Yu L, Zhang X (2019) Improving cross-lingual entity alignment via optimal transport. *IJCAI*, pp 3231–3237
- Pennington J, Socher R, Manning CD (2014) Glove: Global vectors for word representation. In: EMNLP, pp 1532–1543
- Pham H, Xie Q, Dai Z, et al (2021) Meta pseudo labels. In: CVPR, pp 11557–11568
- Raunak V, Gupta V, Metze F (2019) Effective dimensionality reduction for word embeddings. In: The 4th Workshop on Representation Learning for NLP, pp 235–243
- Rizve MN, Duarte K, Rawat YS, et al (2021) In defense of pseudo-labeling: An uncertainty-aware pseudo-label selection framework for semi-supervised learning. In: ICLR

- Sajjadi M, Javanmardi M, Tasdizen T (2016) Mutual exclusivity loss for semi-supervised deep learning. In: ICIP, pp 1908–1912
- Shi W, Gong Y, Ding C, et al (2018) Transductive semi-supervised deep learning using min-max features. In: ECCV 2018, pp 311–327
- Srivastava RK, Greff K, Schmidhuber J (2015) Highway networks. In: ICML Workshop: Deep Learning
- Suchanek FM, Kasneci G, Weikum G (2007) Yago: a core of semantic knowledge. In: WWW, pp 697–706
- Sun K, Zhu Z, Lin Z (2020) Multi-stage self-supervised learning for graph convolutional networks. In: AAAI, pp 5892–5899
- Sun Z, Hu W, Li C (2017) Cross-lingual entity alignment via joint attribute-preserving embedding. In: ISWC, pp 628–644
- Sun Z, Hu W, Zhang Q, et al (2018) Bootstrapping entity alignment with knowledge graph embedding. In: IJCAI, pp 4396–4402
- Tang J, Zhang W, Li J, et al (2023) Robust attributed graph alignment via joint structure learning and optimal transport. arXiv preprint arXiv:230112721
- Tarvainen A, Valpola H (2017) Mean teachers are better role models: Weight-averaged consistency targets improve semi-supervised deep learning results. In: NeurIPS, pp 1195–1204
- Titouan V, Courty N, Tavenard R, et al (2019) Optimal transport for structured data with application on graphs. In: ICML, pp 6275–6284
- Torres LC, Pereira LM, Amini MH (2021) A survey on optimal transport for machine learning: Theory and applications. arXiv preprint arXiv:210601963
- Villani C (2009) Optimal transport: old and new, vol 338. Springer
- Vrandečić D, Krötzsch M (2014) Wikidata: a free collaborative knowledge base. *Communications of the ACM* 57(10):78–85
- Wächter A, Biegler LT (2006) On the implementation of an interior-point filter line-search algorithm for large-scale nonlinear programming. *Mathematical Programming* 106:25–57
- Wang Z, Zhang J, Feng J, et al (2014) Knowledge graph embedding by translating on hyperplanes. In: AAAI, pp 1112–1119
- Wang Z, Lv Q, Lan X, et al (2018) Cross-lingual knowledge graph alignment via graph convolutional networks. In: EMNLP, pp 349–357



- Wu Y, Liu X, Feng Y, et al (2019a) Relation-aware entity alignment for heterogeneous knowledge graphs. In: IJCAI, pp 5278–5284
- Wu Y, Liu X, Feng Y, et al (2019b) Jointly learning entity and relation representations for entity alignment. In: EMNLP/IJCNLP, pp 240–249
- Xu H, Luo D, Carin L (2019a) Scalable gromov-wasserstein learning for graph partitioning and matching. In: NeurIPS, pp 3046–3056
- Xu H, Luo D, Zha H, et al (2019b) Gromov-wasserstein learning for graph matching and node embedding. In: ICML, pp 6932–6941
- Yang H, Zou Y, Shi P, et al (2019) Aligning cross-lingual entities with multi-aspect information. In: EMNLP/IJCNLP, pp 4430–4440
- Yang Y, Lv H, Chen N (2023) A survey on ensemble learning under the era of deep learning. *Artificial Intelligence Review* 56(6):5545–5589
- Yang Z, Qi P, Zhang S, et al (2018) Hotpotqa: A dataset for diverse, explainable multi-hop question answering. In: EMNLP, pp 2369–2380
- Zeng W, Zhao X, Tang J, et al (2020) Collective entity alignment via adaptive features. In: ICDE, IEEE, pp 1870–1873
- Zhang B, Wang Y, Hou W, et al (2021) Flexmatch: Boosting semi-supervised learning with curriculum pseudo labeling. In: NeurIPS, pp 18408–18419
- Zhao X, Zeng W, Tang J, et al (2020) An experimental study of state-of-the-art entity alignment approaches. *IEEE Transactions on Knowledge & Data Engineering* (01):1–1
- Zhu H, Xie R, Liu Z, et al (2017) Iterative entity alignment via knowledge embeddings. In: IJCAI, pp 4258–4264
- Zhu Y, Liu H, Wu Z, et al (2021) Relation-aware neighborhood matching model for entity alignment. In: AAI, pp 4749–4756